Versuch 5: Mechanisches Verhalten von Keramik

Kontakt für Fragen zu diesem Versuch:
Dr. Carlos Pagliosa, NO H19, Tel: 01 632 36 34, carlos.pagliosa@mat.ethz.ch

1. Ziel dieses Praktikumsteils / Zusammenfassung

Dieser Versuch dient dazu, einen kurzen Überblick über die Untersuchungsmethoden und das Verhalten von keramischen Werkstoffen bei Versagen zu geben. Die Weibull-Parameter, welche Aufschluss über die mittlere Festigkeit keramischer Werkstoffe sowie deren Streuung geben, werden im 3-Punkt- sowie im 4-Punkt Biegeversuch bestimmt. Die Auswertung erfolgt graphisch mit Hilfe der Weibull Statistik. Der Zusammenhang zu weiteren Werkstoffkenngrössen wie der Risszähigkeit K_{Ic}, der Härte H, oder dem E-Modul E soll anhand der in der Vorlesung behandelten Modelle (Irwin, Griffith) gebildet werden. Weiter wird der Einfluss von Thermoschock auf die mechanischen Eigenschaften experimentell ermittelt. Für die Versuche werden Proben aus Aluminiumoxid-, Zirkonoxid (TZP)- sowie Glas verwendet. Der nachfolgende Theorieteil (Kap. 2.-5.) dient der Auffrischung des von der Vorlesung bekannten Stoffes zum Thema, und ist Vorbereitung für die praktischen Messungen.
Zum Thema Thermoschock ist eine Publikationen angefügt. Diese soll einen tiefergehenden Einblick in dieses Thema geben. Weitere empfohlene Literatur (Bücher) zum Thema ist im Anhang aufgeführt.

1.1 Durchzuführende Versuche

Biegeversuche zur Bestimmung der Weibull-Parameter

Diese Versuche werden für die folgenden drei Materialien durchgeführt:
- Aluminiumoxid
- Zirkonoxid (TZP)
- Glas

Die Messresultate werden in einem Weibull-Diagramm dargestellt und die Weibullparameter bestimmt.

Vergleich 3-Punkt- mit 4-Punkt-Biegeversuchen

Zum Vergleich der beiden Messgeometrien werden zusätzliche 3-Punkt-Biegeversuche durchgeführt.

Thermoschockverhalten

Das Thermoschockverhalten wird durch Abschrecken im Wasserbad und anschliessendes Messen der Festigkeiten charakterisiert.

Details zu der Versuchsdurchführung werden am jeweiligen Praktikumstermin vermittelt.

2. Theorie: Einleitung

Gegenüber den Metallen und Polymeren verfügen keramische Werkstoffe über einige Eigenschaften wie sie für viele Anwendungen notwendig sind:

- geringe elektrische Leitfähigkeit
- geringe thermische Leitfähigkeit
- gute Festigkeit bei hohen Temperaturen
- Verschleisswiderstand
- Korrosionsbeständigkeit

Dagegen stehen , vorwiegend mechanische, Eigenschaften die nachteilig sind:

- geringe Zugfestigkeit bei Raumtemperatur
- Sprödigkeit
- grosse Streuung der mechanischen Eigenschaften
- unterkritisches Risswachstum

Die Sprödigkeit von Keramik hat ihre Ursache in dem geringen Widerstand gegenüber der Ausbreitung von Rissen, der durch niedrige Werte der Risszähigkeit ausgedrückt wird.
Die grosse Streuung der mechanischen Eigenschaften ist auf die statistische Verteilung der Fehlergrösse und der Fehlerlage zurückzuführen.
Unterkritisches Risswachstum kann nun zu einem Versagen bei konstanter Belastung nach einer bestimmten Betriebszeit führen.

3. Festigkeit

3.1 Allgemeine Betrachtungen

Ein Festkörper verformt sich unter einer von aussen angelegten Spannung zunächst nach dem Hook'schen Gesetz:

$$\sigma = E \cdot \varepsilon \qquad \text{Gl. [1]}$$

Bei Überschreiten einer Grenzspannung (typischerweise im Bereich von 10^{-3} E) treten generell zwei verschiedene Verhalten auf:

a) Der Festkörper versagt spröde, d.h. die während der Verformung angesammelte Verformungsenergie kann nicht durch plastisches Verformen abgebaut werden. Der Körper bricht katastrophal, und die gespeicherte Energie wird in Form von neuen Oberflächen, Wärme und kinetischer Energie frei.
b) Der Festkörper versagt duktil, d.h. die gespeicherte Energie wird durch plastische Verformung und Wärme freigesetzt.

Das Bruchverhalten von Keramik ändert sich mit steigender Temperatur. Bei niedrigen Temperaturen verhält sich die Keramik spröde und die Bruchdehnung beträgt nur ~0.01%. Bei mittleren Temperaturen tritt eine leichte plastische Verformung ein und die Bruchdehnung beträgt zwischen 0.1 und 0.001%. Bei hohen Temperaturen tritt merkliche plastische Verformung ein und die Bruchdehnung beträgt ~1%. Dieser letzte Bereich wird bei Keramiken selten erreicht. Die Übergangstemperaturen sind für verschiedene Arten von Keramiken auch sehr unterschiedlich. So liegt der Übergang vom ersten zum zweiten Bereich für MgO bei 0°C, für SiC bei über 2000°C.

3.2 Griffith-Kriterium zur Beschreibung der Festigkeit

(Zusammenhang: Fehlergrösse <=> Festigkeit)

Anfang des Jahrhunderts wurde entdeckt, dass Fehler im Material die Festigkeit stark herabsetzen. 1920 hat *Griffith* einen Ansatz gefunden, um den Einfluss der Fehler zu beschreiben. Er ging dabei von einem Energiegleichgewicht an der Rissspitze aus, die in einem System mit Riss vorhanden ist und berechnete die Spannung an dem Riss.

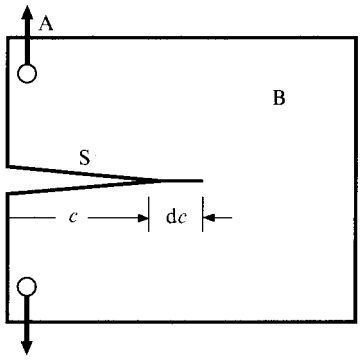

FIG. 1. Modell für den Griffith-Ansatz

Betrachtet man nun die Energie die mit der Schaffung eines neuen Risses in Verbindung gebracht werden kann, wird zwischen *mechanischer Energie(U_M)* und *Oberflächenenergie(U_S)* unterschieden. Die mechanische Energie wiederum besteht aus der im Körper *elastisch gespeicherten Energie(U_E)* und der *potentiellen Energie(U_A)* der von aussen aufgebrachten Kraft.

$$U = U_M + U_S = U_E + U_A + U_S \qquad \text{Gl. [2]}$$

Bei einer Vergrösserung des Risses nimmt, bei gleichbleibender Last, die mechanische Energie ab ($dU_M/dc<0$) und fördert so das Risswachstum. Die Oberflächen die neu geschaffen werden erhöhen die Oberflächenenergie was die Rissausbreitung behindert ($dU_S/dc>0$). Griffith betrachtet nun den Fall, dass die Änderung der Gesamtenergie in Abhängigkeit des Risswachstums gleich Null ist ($dU/dc=0$).

$$U_M = \frac{\pi c^2 \sigma_A^{\,2}}{E'} \qquad \text{Gl. [3]}$$

Aus der linear elastischen Theorie kann man die mechanische Energie des Systems unter konstanter Belastung mit
bestimmen (c ist dabei die Risslänge, σ_A die aussen angelegte Last und E' der E-Modul in der Rissebene). Die Energie, die benötigt wird, um neue Oberflächen zu schaffen, hängt dagegen linear von der Risslänge c ab:

$$U_S = 4c\gamma \qquad \text{Gl. [4]}$$

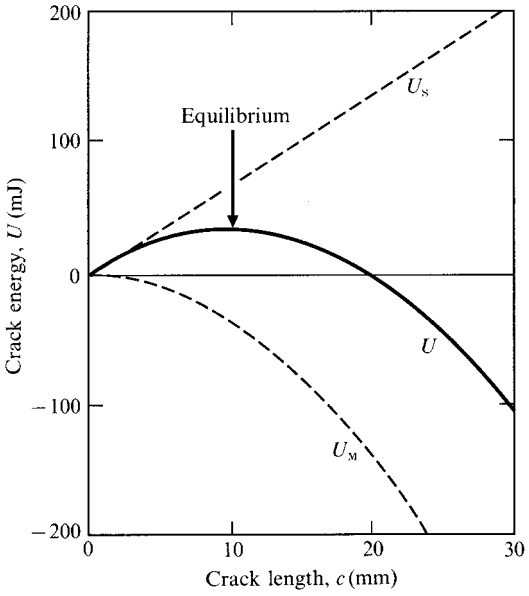

FIG. 2. Energien bei Rissausbreitung unter konstanter Last

Die Gesamtenergie bei einer gegeben Risslänge ist dann bestimmt durch:

$$U(c) = -\frac{\pi c^2 \sigma_A^{\,2}}{E'} + 4c\gamma \qquad \text{Gl. [5]}$$

Leitet man diese Gleichung nach der Risslänge ab um das Gleichgewichtskriterium zu erfüllen, erhält man

$$0 = \frac{-2\pi c \sigma_A^{\,2}}{E'} + 4\gamma \qquad \text{Gl. [6]}$$

Setzt man für σ_A die kritische Spannung ein (z.B. aus Biegebruch Versuchen), bei der das Bauteil versagt, kann man nun die Fehlergösse bestimmen, die bei dieser kritischen Spannung zum Versagen geführt hat. Zu jeder Spannung gehört also eine kritische Fehlergrösse die zum Versagen führt, bzw. zu jedem Fehler gehört eine kritische Spannung bei der das Bauteil zerbricht:

$$\sigma_F = \left(\frac{2 \cdot E'\gamma}{\pi c_0}\right)^{\frac{1}{2}} \qquad \text{Gl. [7]}$$

Dies ist die wichtige *Griffith-Gleichung*. Sie beschreibt wie die Festigkeit σ_F von der Grösse c_0 eines Fehlers abhängt. Sieht man sich diese Gleichung für die Fehlergrösse im Gleichgewichtsfall an, dann wird deutlich, dass für äussere Lasten $\sigma_A<\sigma_F$ der Riss nicht grösser wird und für Lasten $\sigma_A>\sigma_F$ spontan ohne zu stoppen weiterläuft.

Mit der Griffith Beziehung kann man auch die *theoretische Festigkeit* von Materialien abschätzen. Nimmt man als Fehlergrösse den Abstand a_0 zwischen zwei Atomen an, dann erhält man die Festigkeit, die nur durch die Bindungen der Atome bestimmt wird.

$$\sigma_{th} = \left(\frac{2 \cdot E'\gamma}{\pi a_0}\right)^{\frac{1}{2}} \qquad \text{Gl. [8]}$$

Griffith leitete aus seinen Betrachtungen ab, dass die theoretische Festigkeit nur durch die Stärke der Bindungen bestimmt sei und im Bereich von etwa 1/10 des E-Moduls liegt.

3.3 Irwin-Kriterium zur Beschreibung der Festigkeit

(Zusammenhang: Risszähigkeit <=> Festigkeit)

Mit der Griffithgleichung lässt sich die Festigkeit eines Bauteils nur vorhersagen, wenn man den grössten Fehler des Bauteils kennt. Da dies aber nicht der Fall ist, benötigt man eine andere Möglichkeit die Festigkeit zu beschreiben. Idealerweise so, dass sie nur durch Materialeigenschaften beschrieben wird.
Eine andere Art die Vorgänge an einer Rissspitze zu betrachten entwickelte Irwin 1958. Sieht man sich einen Riss an, so konzentrieren sich die Spannungen, die zum Versagen des Materials führen direkt vor der Spitze des Risses. Diese Spannungsüberhöhung lässt sich mit Hilfe des Spannungsintensitätsfaktor beschreiben.
Dazu muss man aber erst einmal die Art der Rissfortpflanzung beschreiben. Man unterscheidet drei verschiedene Arten der Rissausbreitung.

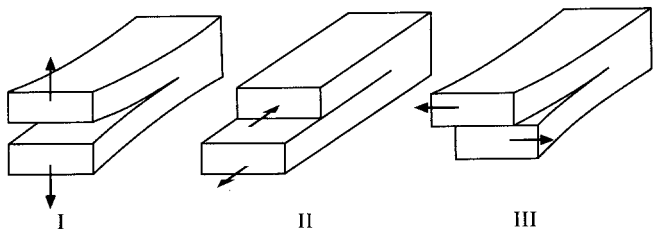

FIG. 3. Rissausbreitungmoden:
Modus I: Zugbeanspruchung senkrecht zur Rissebene
Modus II: Scherbeanspruchung in Rissrichtung
Modus III: Scherbeanspruchung quer zur Rissrichtung

Modus I ist derjenige der für die Betrachtung der Rissausbreitung am wichtigsten ist. Ein Riss versucht immer senkrecht zur maximalen Spannung weiter zu laufen um die Scherspannungen zu minimieren. Deswegen ist der Modus I die bestimmende Art wie ein Riss beeinflusst wird

und damit Versagensbestimmend. Darum ist es für eine einfache Betrachtung des Spannungsfeldes nicht notwendig Modus II und Modus III zu berücksichtigen.

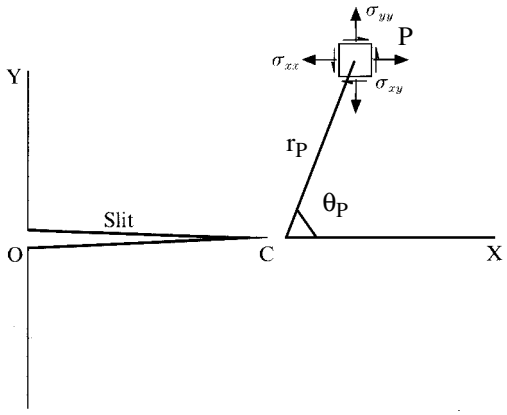

FIG. 4. Spannungsfeld nach Irwin an der Rissspitze mit Koordinatensystem.

Irwin betrachtete nun die Spannungen in einem Punkt P vor der Rissspitze in Abhängigkeit von der Entfernung und der Richtung. Er erhielt dann:

$$\begin{bmatrix}\sigma_{xx}\\ \sigma_{yy}\\ \sigma_{xy}\end{bmatrix}_P = \frac{K_I}{\sqrt{2\pi r}} \cdot \begin{bmatrix}\cos\left(\frac{\theta_P}{2}\right)\cdot\left\{1-\sin\left(\frac{\theta_P}{2}\right)\sin\left(\frac{3\theta_P}{2}\right)\right\}\\ \cos\left(\frac{\theta_P}{2}\right)\cdot\left\{1+\sin\left(\frac{\theta_P}{2}\right)\sin\left(\frac{3\theta_P}{2}\right)\right\}\\ \sin\left(\frac{\theta_P}{2}\right)\cdot\cos\left(\frac{\theta_P}{2}\right)\cdot\cos\left(\frac{3\theta_P}{2}\right)\end{bmatrix} \qquad \text{Gl. [9]}$$

Betrachtet man die Energierate, mit der die Energie bei der Neubildung eines Risses freigesetzt wird, dann erhält man diese über den Unterschied der Rissenergie zu Beginn des Risses und aus der Energie wenn der Riss um Δx weitergelaufen ist.

$$G \equiv \lim_{\Delta x \to 0} \frac{2}{\Delta x} \int_0^{\Delta x} \frac{\sigma_{yy}(\Theta = 0)}{2} u_y(\Theta = \pi)\, dx \qquad \text{Gl. [10]}$$

wobei σ_{yy} die Spannung senkrecht zur Rissausbreitung ist und u_y die Rissöffnung von der Mitte der Rissebene aus darstellt (2u ist die gesammte Rissbreite). Indem man dieses Integral löst erhält man:

$$G = \frac{K_I^2}{E} \qquad \text{Gl. [11]}$$

Diese freigesetzte Energie kann man aber auch aus der mechanischen Energie über die Rissverlängerung ableiten:

$$G = -\frac{dU_M}{dc} \qquad \text{Gl. [12]}$$

Unter konstanter Last gilt:

$$U_M = -U_E = \frac{\pi\sigma_A^2 c^2}{E} \qquad \text{Gl. [13]}$$

Setzt man die drei Gleichungen zusammen und gruppiert die Konstanten, so erhält man für den Spannungsintensitätsfaktor

$$K_I = Y \cdot \sigma_A \cdot \sqrt{c} \qquad \text{Gl. [14]}$$

K_I hängt also neben der aufgebrachten äusseren Spannung und der Fehlergrösse auch von einem Geometriefaktor ab, der durch die Form des Risses bestimmt wird.

Gerader Riss, unendlich grosse Probe	$Y = \sqrt{\pi}$
Kantenriss	$Y = 1.12 \cdot \sqrt{\pi}$
"Penny"-Riss	$Y = \frac{2}{\sqrt{\pi}}$

Werte für Geometriefaktoren in der Irwinbeziehung.

Der Spannungsintensitätsfaktor gibt uns also eine Aussage über die Intensität und die Verteilung eines Spannungsfeldes das durch einen gegeben Fehler entsteht.
Wird die Probe mit immer höheren Spannungen belastet nimmt der Spannungsintensitätsfaktor immer weiter zu. Sobald die von aussen angelegte Spannung die maximale Festigkeit erreicht hat wird der Riss instabil. An dieser Stelle erreicht der Spannungsintensitätsfaktor einen kritischen Wert der von einer weiteren Zuhname der Spannung unabhängig ist. Man nennt diesen Wert den *kritischen Spannungsintensitätsfaktor* K_{Ic}, oder *Risszähigkeit* bzw. *Bruchzähigkeit*. Dieser K_{Ic}-Wert ist eine experimentell ermittelbare Werkstoffkenngrösse mit der Einheit $[K_{Ic}]$=MPa√m

Mittels des kritischen Spannungsintensitätsfaktors und der Bruchspannung lässt sich die Grösse des Fehlers abschätzen der zum Bruch der Probe geführt hat:

$$c = \left(\frac{K_{Ic}}{\sigma_c Y}\right)^2 \qquad \text{Gl. [15]}$$

Der K_{Ic} ist ein Mass dafür, wie gut ein Werkstoff der Verlängerung eines Risses widerstehen (materialspezifisch) und so einen Bruch vermeiden kann. Je höher die Risszähigkeit ist, desto schwieriger ist es für einen Riss, sich durch das Material zu bewegen.
Vor allem bei Aluminiumoxid und Zirkonoxid ist das Phänomen bekannt, dass die Bruchzähigkeit mit fortschreitenden Riss steigt. Dies geschieht normalerweise durch Verzweigung des Risses an der Risspitze (Mikrorisse).

Typische Risszähigkeiten für Keramiken sind:

Al_2O_3	3.5...5
Si_3N_4 (reaktionsgesintert, RBSN)	1.9...3.2
SiC (heissgepresst, HP)	3.8...5
ZrO_2 (Mgo-teilstabilisiert)	7...12

Für die Anwendung von Keramiken ist eine Steigerung der Zähigkeit sinnvoll und notwendig. Man kann zwei unterschiedliche Gruppen von zähigkeitssteigernden Mechanismen unterscheiden. Die Prozesse der ersten Gruppe laufen vor der Risspitze ab, die der zweiten Gruppe hinter der Risspitze.

Gruppe I enthält:
- Phasenumwandlungen -> Volumenzunahme (z.B. Y-TZP)
- Bildung von Mikrorissen
- Rissablenkung
- Rissverzweigung
- Spannungsfelder durch Phasen mit unterschiedlichen thermischen
- Ausdehnungskoeffizienten
- Plastische Fliessprozesse bei hohen Temperaturen

Gruppe II besteht aus folgenden Mechanismen:
- Mechanische Verzahnung
- Brückenbildung durch Verstärkungsphasen (z.B. durch Fasern)
- Reibungseffekte der neu gebildeten Rissoberflächen
- Restdruckspannungen durch Mikrorissbildung
- Erhöhte Nachgiebigkeit der vor der Rissfront gebildeten Zone durch Mikrorisse

4. Statistische Festigkeitstheorie (Weibull-Statistik)

Wenn man die Festigkeit von Keramik misst, stellt man fest, dass die Werte sehr stark streuen, unabhängig davon dass die Geometrie der Proben identisch war.

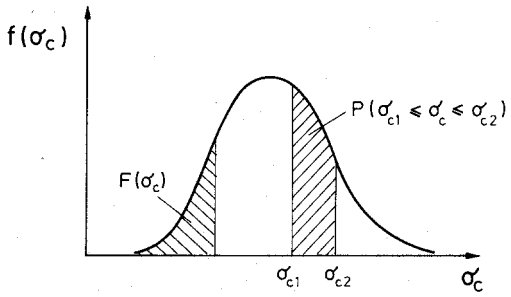

FIG. 5. Verteilungsdichte der Festigkeit bei einer Reihe gemessener Bauteile

Die Verteilung der Festigkeiten hat drei wichtige Eigenschaften:

1. Das Integral über den gesamten Bereich der Festigkeit ist gleich eins:

$$\int_0^\infty f(\sigma_c)d\sigma_c = 1 \qquad \text{Gl. [16]}$$

1. Das Integral zwischen zwei Werten σ_{c1} und σ_{c2} entspricht der Wahrscheinlichkeit, dass die Festigkeit zwischen diesen Werten liegt:

$$P(\sigma_{c1} < \sigma_c < \sigma_{c2}) = \int_{\sigma_{c1}}^{\sigma_{c2}} f(\sigma_c)d\sigma_c \qquad \text{Gl. [17]}$$

1. Die Wahrscheinlichkeit dass die Festigkeit kleiner als σ_c ist, lautet:

$$F(\sigma_c) = \int_o^{\sigma_c} f(\sigma_c)d\sigma_c \qquad \text{Gl. [18]}$$

Die Festigkeit wird durch den grössten Fehler innerhalb eines Bauteils bestimmt. Diese maximalen Fehler sind aber nicht in allen Bauteilen gleich gross sondern unterliegen einer Grössenverteilung, die ebenfalls normiert ist.

$$\int_0^\infty f(a)da = 1 \qquad \text{Gl. [19]}$$

1939 hat sich Weibull daran gemacht eine Methode zu entwickeln, mit der man die Streuung der Festigkeiten beschreiben kann und eine Vorhersage über das Festigkeitsverhalten von Bauteilen aus einer Messreihe machen kann.
Betrachtet man ein Bauteil, das eine bestimmte Anzahl Fehler pro Volumeneinheit hat (z ist die Fehlerdichte) dann ist die mittlere Anzahl der Fehler im Gesamtvolumen

$$Z = zV \qquad \text{Gl. [20]}$$

Die wirkliche Fehlerzahl kann aber grösser oder kleiner sein. Die Wahrscheinlichkeit, dass ein Bauteil M Fehler besitzt lässt sich durch eine Poissonverteilung beschreiben:

$$P(M) = \frac{e^{-Z} Z^{M}}{M!} \qquad \text{Gl. [21]}$$

Durch Umformen und unter Hinzunahme der Verteilung der maximalen Fehler erhält man die Wahrscheinlichkeit für das Auftreten eines Fehlers einer bestimmten Grösse

$$H(a) = \exp[-zV(1 - F(a))] \qquad \text{Gl. [22]}$$

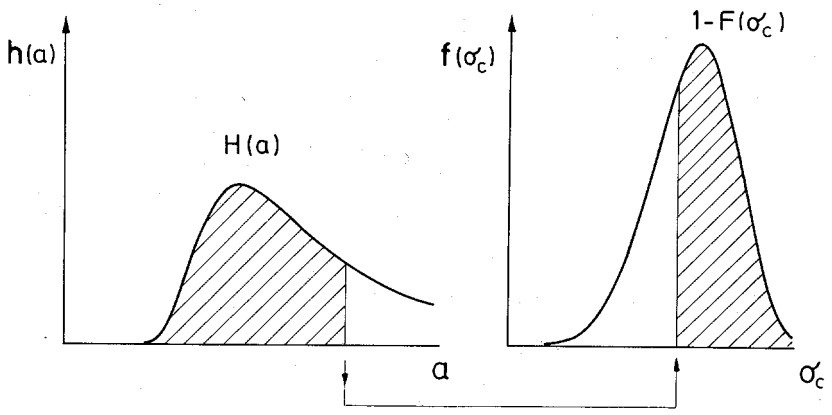

Verteilungsdichte des maximalen Fehlers und der Festigkeit

Über die Irwin-Beziehung lässt sich die Verteilung des maximalen Fehlers nun mit der Verteilung der Spannungen korrelieren. Daraus folgt, dass

$$1 - F(\sigma_c) = H(a) \qquad \text{Gl. [23]}$$

Entscheidend für die Verteilung von a_{max} und σ_c ist der Verlauf von f(a) bei grossen Werten. Dies kann man durch ein Potenzgesetz annähern

$$f(a) \sim \frac{1}{a^{r}} \qquad \text{Gl. [24]}$$

daraus folgt,dass

$$F(\sigma_c) = 1 - \exp[-zv(1 - F(a))] \quad \text{Gl. [25]}$$

Die Verteilungsfunktion F(a) ergibt sich dann als

$$F(a) = 1 - \left(\frac{a_0}{a}\right)^{r-1} \quad \text{Gl. [26]}$$

Diese Gleichung hat die Randbedingung, dass a nicht kleiner als a_0 sein darf.
Für die Verteilung der Festigkeit ergibt sich damit dann

$$F(\sigma_c) = 1 - \exp\left[-\left(\frac{\sigma_c}{\sigma_0}\right)^m\right] \quad \text{Gl. [27]}$$

$$F(\sigma_c) = 1 - \exp\left[-zV\left(\frac{a_0 {\sigma_c}^2 Y^2}{{K_{Ic}}^2}\right)^{r-1}\right] \quad \text{Gl. [28]}$$

Diese Verteilung nennt man auch die *Weibull-Verteilung der Festigkeiten*.

4.1 Die Weibullparameter

Um die Weibull-Verteilung einfacher nutzen zu können wird sie häufig doppelt logarithmisch dargestellt.

$$\ln\ln\frac{1}{1-F} = m\ln\sigma_c - m\ln\sigma_0 \quad \text{Gl. [29]}$$

Dies bedeutet dass man bei der Auftragung von lnln1/(1-F) gegen $\ln\sigma_c$ eine Gerade mit der Steigung m erhält, deren Lage durch $\ln\sigma_0$ bestimmt ist.

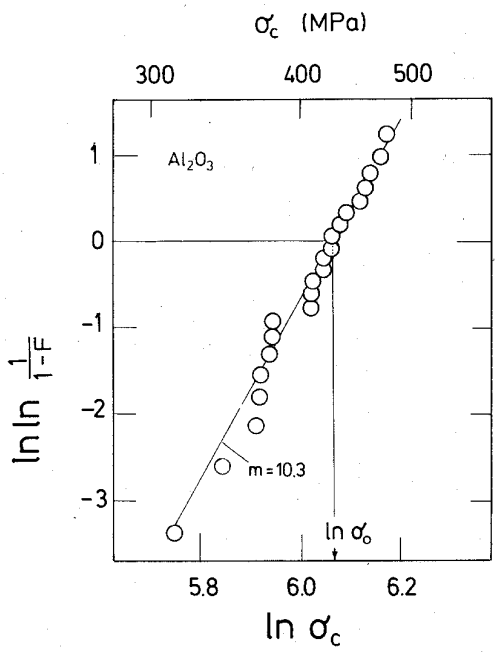

Darstellung der Streuung der Festigkeiten von Aluminiumoxid mit der Weibull-Verteilung

Die beiden Weibullparameter m und σ_0 haben folgende Bedeutung:

- m ist ein Mass für die Streuung der Festigkeitswerte. Je grösser m ist, desto enger liegen die gemessenen Festigkeiten zusammen. Je enger die Festigkeitswerte zusammen liegen, desto genauer kann man eine Vorhersage über die Belastung treffen,bei welchen ein Bauteil der gleichen Machart versagen wird. Man spricht dann von *Zuverlässigkeit*. Je höher m desto zuverlässiger wird die Vorhersage.

- σ_0 ist der Wert bei der 63.2% (= 1 - 1/e ...) aller Proben versagen. Diese Kennzahl wird auch *mittlere Festigkeit* genannt.In der doppelt-logarithmischen Weibull-Auftragung ist σ_0 der Wert wo lnln[1/(1-F)]=0 ist.

4.2 Anleitung für die Weibull-Auswertung

In diesem Abschnitt soll die Vorgehensweise zur Ermittlung der Weibull Parameter m und σ_0 Schritt für Schritt beschrieben werden:

1. Zuerst muss man die Festigkeitswerte von mindestens 10 Proben ermitteln. Die Präparation und das Material der Proben muss bei allen gleich sein. Je höher die Anzahl der Proben ist, desto genauer wird die Statistik. Zur Ermittlung der Festigkeit kann man die Biegebruchanordnung benutzen.
1. Die gemessenen Festigkeitswerte werden der Grösse nach geordnet und jeder Wert mit einer Ordnungszahl versehen. Bei N Proben erhält die Probe mit den niedrigsten Festigkeits die Zahl 1 und die mit dem höchsten Festigkeitswert die Zahl N.

1. Die Versagenswahrscheinlichkeit hängt von der Anzahl der Proben und von ihrem Platz innerhalb der Reihe ab.

$$F_i = \frac{i - 0.5}{n} \qquad \text{Gl. [30]}$$

i ist hierbei der i-te Wert innerhalb der Reihe.

1. Alle Festigkeitswerte σ_c werden als $\ln\sigma_c$ gegen $\ln\ln 1/(1\text{-}F)$ aufgetragen. Die Werte werden durch eine Ausgleichsgerade verbunden. Die Steigung der Ausgleichsgeraden ist der Weibullparameter m und der Wert der Geraden beim Punkt $\ln\ln[1/(1\text{-}F)]=0$ ist der Wert $\ln\sigma_0$

4.3 Der Grösseneinfluss der Proben

Volumenabhängigkeit der Festigkeit

Aus der oben angeführten Weibull-Verteilung kann man den Grösseneinfluss der Proben auf die Festigkeitsverteilung erkennen:

$$F(\sigma_c) = 1 - \exp\left[-zV\left(\frac{a_0 {\sigma_c}^2 Y^2}{{K_{Ic}}^2}\right)^{r-1}\right] \qquad \text{Gl. [31]}$$

Für eine festgelegte Versagenswahrscheinlichkeit F kann man nun das Verhältniss der Festigkeiten zweier unterschiedlich grosser Körper gleicher Form bestimmen:

$$\frac{\sigma_1}{\sigma_2} = \left(\frac{V_2}{V_1}\right)^{\frac{1}{m}} \qquad \text{Gl. [32]}$$

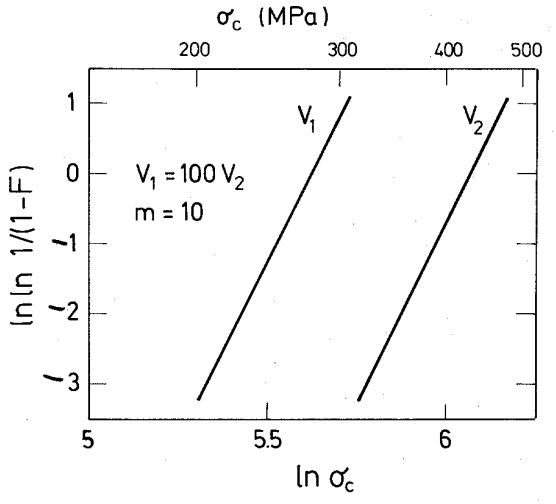

Einfluss des Volumens auf die Verteilung der Festigkeit;
kleinere Proben haben die höhere Festigkeit

Bei allen bisherigen Betrachtungen wurden immer Volumenfehler angenommen. Für Oberflächenfehler gelten genau die selben Abhängigkeiten. Statt der Volumina müssen dann die entsprechenden Oberflächen eingesetzt werden.

4.4 Vergleich 3-Punkt und 4-Punkt-Biegeversuch

Der Biegebruchversuch ermöglicht es, die Bruchfestigkeit unter Zugspannung zu bestimmen, ohne dass eine spezielle Probengeometrie wie beim Zugversuch notwendig ist. Während beim Zugversuch noch eine besondere Form der Probe an den Enden notwendig ist und so der Querschnitt über die gesamte Länge der Probe nicht konstant bleibt, kann man im Biegebruchversuch rechteckige oder runde Stäbe brechen, deren Herstellung vergleichsweise einfach ist.

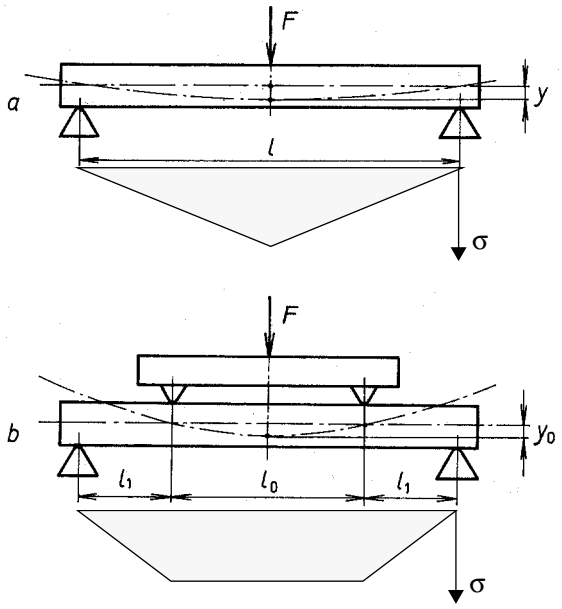

Schema für (a) Drei-Punkt-Biegung und (b) Vier-Punkt-Biegung. Die Flächen unter den Balken geben den Verlauf der Zugspannung an der Unterseite der Proben wieder

Die Spannung an der Unterseite der Proben (maximale Zugspannung) lässt sich über die Last *F* mit der die Probe belastet wird und der Geometrie der Probe bestimmen. Für rechteckige Proben gilt dann bei der Vier-Punkt-Biegung:

$$\sigma = \frac{3 \cdot l_1}{W^2 \cdot B} \cdot F \qquad \text{Gl. [33]}$$

mit *W* als Probenhöhe und *B* als Probenbreite. Für Proben mit rundem Querschnitt gilt (Vier-Punkt-Biegung):

$$\sigma = \frac{2 \cdot l_1}{\pi \cdot r^3} \cdot F \qquad \text{Gl. [34]}$$

Für den Fall der Drei-Punkt-Biegung können die gleichen Formeln analog verwendet werden, wobei l_1 durch den halben Abstand der äusseren Auflager $l/2$ ersetzt wird.
Beim Biegebruchversuch tauchen kleine Fehler durch Effekte an den Probenauflagern auf: Durch Reibung an den Auflagern und den Drucklagern können zusätzliche Kräfte durch Reibung übertragen werden und entstehen. Dieser Effekt lässt sich aber durch bewegliche Auflager minimieren.
Wenn sich die Probe durchbiegt verändert sich der Abstand der Auflager auf der Probenunterseite. Dieser Effekt ist aber nicht sehr gross (Abweichungen von unter 1%) und lässt sich durch die Auflagergrösse steuern.
Die inneren Drucklager können die Kraft nicht ganz spannungsfrei übertragen, so dass Zugspannungen direkt an den Lagern entstehen die sich mit den Biegespannungen überlagern. Dies kann zu einer Abweichung der maximalen Spannung von bis zu 2.3% führen. Dieser Effekt ist bei der Drei-Punkt-Biegung grösser als bei der Vier-Punkt-Biegung. Der Vier-Punkt-Biegung wird im allgemeinen wegen des grösseren Bereichs mit konstantem Biegemoment der Vorzug gegeben. Die gemessenen Werte liegen aufgrund der Versuchsanordnung niedriger als bei der Drei-Punkt Biegung. Deswegen kann man Festigkeitswerte nur vergleichen wenn man die Messmethode weiss mit der sie gemessen wurden.

5. Thermoschockverhalten

Keramische Stoffe sind thermoschockempfindlich. Wenn sie zu grossen und zu plötzlichen Temperaturänderungen und Gradienten ausgesetzt sind, dann kann es zum Versagen kommen. Durch Temperaturänderungen kommt es zu thermischen Dehnungen im Körper

$$\varepsilon_{th} = \alpha(T_1 - T_0) \qquad \text{Gl. [35]}$$

wobei α der Wärmeausdehnungskoeffizient ist und T_1 grösser als T_0. Wenn die thermische Ausdehnung des Bauteils behindert ist (Einspannung), treten elastische Dehnungen auf, welche die thermischen Dehnungen kompensieren

$$\varepsilon_{th} + \varepsilon_{el} = 0 \qquad \text{Gl. [36]}$$

Dies wiederrum führt zu Spannungen die, falls sie die Bruchfestigkeit des Körpers überschreiten, zum Versagen führen

$$\sigma_{th} = E\varepsilon_{el} = -E\varepsilon_{th} = -E\alpha(T_1 - T_0) \qquad \text{Gl. [37]}$$

Die Thermoschockempfindlichkeit wird gemessen indem man Proben auf eine Temperatur T_1 aufheizt und dann auf eine Temperatur T_0 abschreckt. Danach wird die Festigkeit der Proben gemessen.

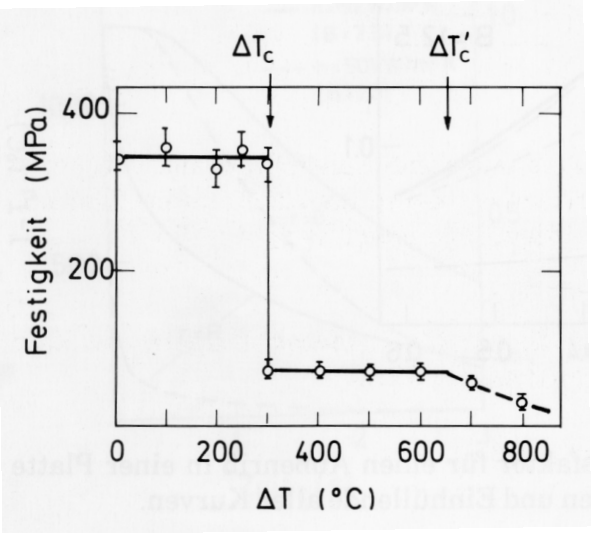

Bild 4-1: Festigkeit von thermogeschockten Biegeproben aus Al_2O_3.

Die Thermoschockempfindlichkeit kann mittels verschiedener Parameter beschrieben werden, die je nach den vorgegebenen Randbedingungen gültig sind.
Für unendlich grossen Wärmeübergang gilt

$$R_s = \frac{\sigma_c(1-\nu)}{\alpha E} \qquad \text{Gl. [38]}$$

wobei ν die Querkontraktionszahl ist. Der Parameter R_S beschreibt die Empfindlichkeit des Bauteils gegenüber der Temperaturänderung. Je kleiner R_S ist, desto grösser wird die Thermoschockempfindlichkeit.
Bei konstantem Wärmeübergang wird die Formel mit der Wärmeleitfähigkeit erweitert.

$$R'_s = \frac{\lambda\sigma_c(1-\nu)}{\alpha E} = \lambda R_S \qquad \text{Gl. [39]}$$

Ist ein konstante Aufheizrate an der Oberfläche vorgegeben, enthält der Werkstoffparameter Thermoschockempfindlichkeit zusätzlich noch die Dichte und die Wärmekapazität des Werkstoffes

$$R_S'' = \frac{\lambda\sigma_c(1-\nu)}{\alpha E\rho C_p} = \frac{R_S'}{\rho C_p} = \frac{\lambda R_S}{\rho C_p} \qquad \text{Gl. [40]}$$

6. Kontrollfragen

- Weshalb haben gemessenen Festigkeiten bei Keramik eine grössere Streuung als bei Metallen?
- Wie hängt die Festigkeit von der Fehlergrösse ab? Wer hat diesen Zusammenhang als erster erkannt?
- Welche Fehler gibt es in Keramik? Woher kommen diese Fehler?
- Wie kann man die Zähigkeit erhöhen?
- Wie funktioniert die Zähigkeitserhöhung beim TZP?
- Weshalb die zweifach logarithmische Darstellung im Weibull-Diagramm?
- Weshalb ist die mittlere Festigkeit abhängig vom Volumen der Probe?
- Wieso ist die Oberflächengüte der Proben wichtig?
- Vergleich von 3-Punkt und 4-Punkt-Biegeversuch: In welcher Messgeometrie werden höhere mittlere Festigkeiten gemessen? Erklärung?

7. Literatur

1. Vorlesungsskript Ingenieurkeramik I; Prof.L.J.Gauckler; Nichtmetallische Werkstoffe; ETH Zürich

2. Munz D., Fett T. "Mechanische Verhalten keramischer Werkstoffe" Springer Verlag, Berlin (1989) [Keramik-Bibliothek: MEI-1989-5726]

   oder neue englische Ausgabe: "Ceramics: Mechanical Properties, Failure Behaviour, Materials Selection" Springer-Verlag, Berlin (2001) [Keramik-Bibliothek: MEI-2001-7029]

3. Green, D.J. "An introduction to the mechanical properties of ceramics" Cambridge University Press, Cambridge, UK (1998) [Keramik-Bibliothek: MEI-1998-6740]

4. Kingery, W.D. "Factors affecting thermal shock resistance of ceramic materials" *Journal of the American Ceramic Society* **38**, 3-15 (1955) [im Anhang

Factors Affecting Thermal Stress Resistance of Ceramic Materials

by W. D. KINGERY

Ceramics Division, Department of Metallurgy, Massachusetts Institute of Technology, Cambridge, Massachusetts

The sources and calculation of thermal stresses are considered, together with the factors involved in thermal stress resistance factors. Properties affecting thermal stress resistance of ceramics are reviewed, and testing methods are considered.

I. Introduction

THE susceptibility of ceramic materials to thermal stresses has been recognized for a long time. More than one hundred years ago equations for the thermal stresses arising from temperature gradients in a cylinder were derived by Duhamel (1838).[1] Since that time, about thirty papers have appeared which mainly consider the calculation of thermal stresses in an infinite cylinder subjected to temperature gradients. It is apparent that thermal stresses are not a new or uninvestigated phenomenon.

The first quantitative treatment of thermal stress fracture in ceramic materials was prepared by Winkelmann and Schott (1894).[2] Hovestadt and Everhart (1902)[3] gave a correct solution for the case of infinitely rapid cooling. A number of investigators considered testing methods for glasses and for refractories and their correlation with service results. Norton (1926)[4] studied the problem and first suggested that shear stresses must be considered as well as tensile stresses. More recently, several investigators, particularly those interested in special refractory applications, have considered the problem of thermal stresses from both theoretical and experimental points of view. New attempts have been made to define and to measure a material property which can be called "resistance to thermal stresses." Although these attempts have not been completely successful in a quantitative way, they have led to a much improved understanding of the factors that contribute to thermal stress resistance. It is the purpose of the present paper to consider these factors and their effect on thermal stress resistance.

Presented at the Symposium on Thermal Fracture sponsored by the New England Section, The American Ceramic Society, at Massachusetts Institute of Technology, Cambridge, Massachusetts, on September 16, 1953. Received April 20, 1954.

The author is assistant professor of ceramics, Ceramics Division, Department of Metallurgy, Massachusetts Institute of Technology.

[1] J. M. C. Duhamel, "Memoire sur le calcul des actions moleculaires developpers par les changements de temperature dans les corps solides," *Memoirs . . . de l'institute de France*, V, 440 (1838).

[2] A. Winkelmann and O. Schott, "Ueber thermische Widerstandscoefficienten vershiedener Gläser in ihrer Abhängigkeit von der chemischen Zusammensetzung," *Ann. Physik. Chem.*, 51, 730 (1894).

[3] H. Hovestadt and J. D. Everhart, Jena Glass, Macmillan Co., New York, 1902, p. 228.

[4] F. H. Norton, "Mechanism of Spalling," *J. Am. Ceram. Soc.*, 9 [7] 446–61 (1926); "A General Theory of Spalling," *ibid.*, 8 [1] 29–39 (1925).

II. Nomenclature

The nomenclature and letter symbols employed in the consideration of thermal stresses have varied considerably. In this paper the following definitions will be employed:

Thermal stress: A stress arising from a temperature gradient.
Thermal stress resistance: Resistance to weakening or to fracture from thermal stresses.
Spalling: The breaking away of pieces of a shape or structure.
Thermal spalling: Spalling caused by thermal stresses.
Thermal fracture: Fracture caused by thermal stresses.
Thermal endurance: Resistance to weakening or fracture when subjected to conditions causing thermal stresses.
Thermal shock: A sudden transient temperature change.
Thermal shock resistance: Resistance to weakening or fracture when subjected to thermal shock.

III. Origin and Calculation of Thermal Stresses

The origin of thermal stresses is the difference in thermal expansion of various parts of a body under conditions such that free expansion of each small unit of volume cannot take place.[5] This condition can arise in a number of ways.

(1) Stresses Arising at Uniform Temperature

If a ceramic body is changed from an initial temperature, t_0, to a new uniform temperature, t', no stresses arise providing that the body is homogeneous, isotropic, and unrestrained (free to expand). Under these conditions, the linear expansion of each volume element is $\alpha(t' - t_0)$ and the shape of the body is unchanged.

If the body is not homogeneous and isotropic, as in a polycrystalline material with anisotropic crystals or in a mixture of two materials (such as a glass-mullite porcelain), stresses will arise due to the difference in expansion between crystals or phases. The magnitude of the stresses will depend on the elastic properties and expansion coefficients of the components. These "microstresses" or "tessellated stresses" have been thoroughly investigated in connection with magnetic and fatigue properties.[6] In extreme cases they may lead to serious weakening or fracture.[7] A similar effect on a larger scale is the stresses caused by differences of expansion between a

[5] S. Timoshenko, Theory of Elasticity, McGraw-Hill Book Co., Inc., New York, 1934. 415 pp.

[6] (*a*) F. László, "Tessellated Stresses," *J. Iron Steel Inst.* (London), **148** [1] 173–99 (1943).
(*b*) F. P. Bowden, "Experiments of Boas and Honeycombe on Internal Stresses Due to Anisotropic Thermal Expansion of Pure Metals and Alloys," *J. Inst. Metals, Symposium on Internal Stresses in Metals and Alloys*, Preprint No. 1100, 6 pp. (1947).
(*c*) J. P. Nielsen and W. R. Hibbard, Jr., "X-ray Study of Thermally Induced Stresses in Microconstituents of Aluminum-Silicon Alloys," *J. Appl. Phys.*, 21, 853–54 (1950).

[7] (*a*) N. N. Ault and H. F. G. Ueltz, "Sonic Analysis for Solid Bodies," *J. Am. Ceram. Soc.*, 36, [6] 199–203 (1953).
(*b*) W. R. Buessem, N. R. Thielke, and R. V. Sarakauskas, "Thermal Expansion Hysteresis of Aluminum Titanate," *Ceram. Age*, 60 [5] 38–40 (1952).

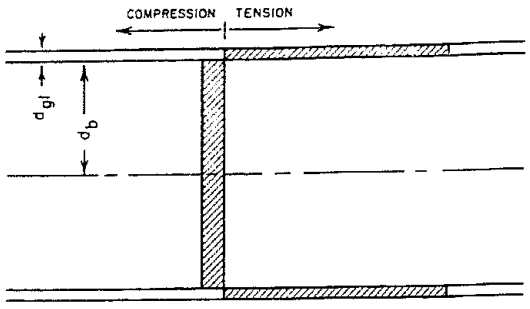

Fig. 1. Stresses in glaze on infinite slab.

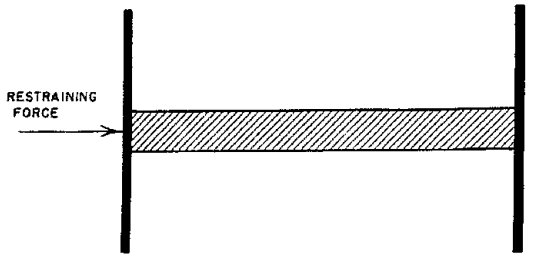

Fig. 2. Restraint of expansion by fixed supports.

glaze or enamel and the underlying ceramic or metal. If stress-free at t_0, the stresses will depend on the new temperature, t', on the elastic properties, and on the coefficients of expansion. For a thin glaze on an infinite slab, the stresses will be as shown in Fig. 1. The stresses[8] are given in equations (1) and (2) for the simplest case where the elastic properties of glaze and body are the same.

[8] (*a*) J. N. Goodier, "On the Integration of Thermo-elastic Equations," *Phil. Mag.*, **23**, 1017 (1937).
(*b*) W. M. Hampton, "Study of Stresses in Flashed Glasses," *J. Soc. Glass Technol.*, **20**, 273 (1936).

Table I. Surface and Center Stresses in Various Shapes

Shape	Surface	Center
Infinite slab	$\sigma_z = 0$ $\sigma_y = \sigma_z = \frac{E\alpha}{(1-\mu)}(t_a - t_s)$	$\sigma_z = 0$ $\sigma_y = \sigma_z = \frac{E\alpha}{(1-\mu)}(t_a - t_c)$
Thin plate	$\sigma_y = \sigma_z = 0$ $\sigma_z = \alpha E(t_a - t_s)$	$\sigma_y = \sigma_z = 0$ $\sigma_z = \alpha E(t_a - t_c)$
Thin disk	$\sigma_r = 0$ $\sigma_\theta = \frac{(1-\mu)E\alpha}{(1-2\mu)}(t_a - t_s)$	$\sigma_r = \frac{(1-\mu)E\alpha}{2(1-2\mu)}(t_a - t_c)$ $\sigma_\theta = \frac{(1-\mu)E\alpha}{2(1-2\mu)}(t_a - t_c)$
Long solid cylinder	$\sigma_r = 0$ $\sigma_\theta = \sigma_z = \frac{E\alpha}{(1-\mu)}(t_a - t_s)$	$\sigma_r = \frac{E\alpha}{2(1-\mu)}(t_a - t_c)$ $\sigma_\theta = \sigma_z = \frac{E\alpha}{2(1-\mu)}(t_a - t_c)$
Long hollow cylinder	$\sigma_r = 0$ $\sigma_\theta = \sigma_z = \frac{E\alpha}{(1-\mu)}(t_a - t_s)$	$\sigma_r = 0$ $\sigma_\theta = \sigma_z = \frac{E\alpha}{(1-\mu)}(t_a - t_c)$
Solid sphere	$\sigma_r = 0$ $\sigma_t = \frac{E\alpha}{(1-\mu)}(t_a - t_s)$	$\sigma_t = \sigma_r = \frac{2E\alpha}{3(1-\mu)}(t_a - t_c)$
Hollow sphere	$\sigma_r = 0$ $\sigma_t = \frac{\alpha E}{(1-\mu)}(t_a - t_s)$	$\sigma_r = 0$ $\sigma_t = \frac{\alpha E}{(1-\mu)}(t_a - t_c)$

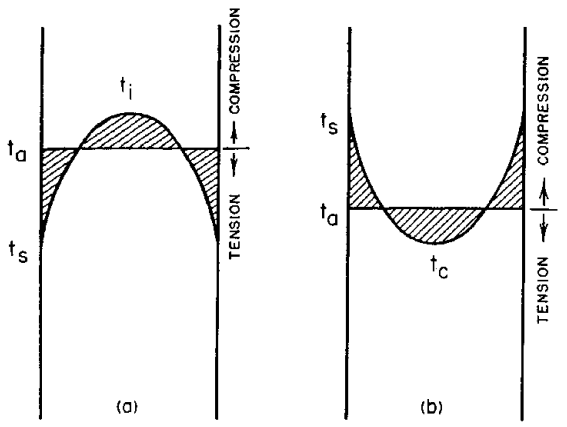

Fig. 3. Temperature and stress distribution for (*a*) cooling and (*b*) heating a slab.

$$\sigma_{gl} = E(t_0 - t')(\alpha_{gl} - \alpha_b)(1 - j)(1 - 3j + 6j^2) \quad (1)$$

$$\sigma_b = E(t_0 - t')(\alpha_b - \alpha_{gl})(j)(1 - 3j + 6j^2) \quad (2)$$

where $j = d_{gl}/d_b$.

Similarly, if a bar of material is completely restrained from expanding by application of restraining forces due to the design of a part, stresses arise as for Fig. 2, where

$$\sigma = \frac{E\alpha(t_0 - t')}{(1 - \mu)} \quad (3)$$

Stresses such as these, although not due to a temperature gradient and therefore not classified as thermal stresses as the term has been defined here, will be additive with any thermal stresses developed and must be considered in any practical applications of thermal stress resistance.

(2) *Stresses Arising from Temperature Gradients*[5]

A temperature gradient does not necessarily give rise to thermal stresses. For instance, in an infinite slab with a linear temperature gradient, the body can expand without incompatible strains and no stresses arise. In general, however, the temperature is not a linear function of dimension and free expansion of each volume element would lead to separation of the elements so that they could not be fitted together. Since they are constrained in the same body, stresses arise which can be exactly calculated for a number of purely elastic bodies from the theory of elasticity. Without going into these calculations in detail, it can be shown that for symmetrical temperature distributions, the stresses resulting for simple shapes are those given in Table I. The stress at any point is determined by the temperature distribution, by the shape of the body, and by the physical constants E, α, and μ, which are taken as independent of temperature. If these factors are known, the stress can be calculated at any point for sufficiently simple shapes.

The temperature and stress distribution for heating and cooling the surface of an infinite slab at a constant rate is shown in Fig. 3. On cooling, the maximum stress is the tensile stress on the surface and the center is in compression. On heating, the maximum stress is the compressive stress on the surface, and the center is in tension. There also are shear stresses equal to

half the difference between the principal stresses. These shear stresses are equal during heating and cooling, and are maximum at the surface. For nonsymmetrical temperature distributions, there are also bending stresses (which can be calculated from elastic theory).[5]

IV. Temperature Distribution

It is clear that in order to calculate thermal stresses a knowledge of the temperature distribution is necessary. Two cases can be considered.

(1) *Steady State*[9]

In the steady state the temperature distribution is determined by the rate of heat flow, by the specimen shape, and by the thermal conductivity. In a hollow cylinder, for example, the temperature distribution is logarithmic. For simple shapes the distribution can be obtained by integration of the heat flow equation containing the thermal conductivity as a material property relating heat flow and temperature gradient,

$$q = -kA\frac{dt}{dx} \tag{4}$$

This may be integrated for k as a function of temperature, but k is generally taken as a constant mean value. For complex shapes not susceptible to analytical treatment, numerical methods are available which allow the calculation of temperature distribution to any desired accuracy.[9(b), 10]

(2) *Unsteady or Transient State*[9, 10]

In this case the temperature at any point changes with time, in a manner depending on the thermal conductivity, k, and on the heat capacity per unit volume (ρc_p), as follows:

$$\frac{dt}{d\theta} = \frac{k}{\rho c_p}\left(\frac{\partial^2 t}{\partial x^2} + \frac{\partial^2 t}{\partial y^2} + \frac{\partial^2 t}{\partial z^2}\right) \tag{5}$$

This equation applies strictly only when k, ρ, and c_p are independent of temperature, position, and direction. If k or c_p is not constant, an analytical solution is usually not possible, but numerical or analogue methods can be employed in these cases.[10]

In determining temperature at various times by analytical methods, somewhat arbitrary boundary conditions must be assumed. Well-known solutions are available for the cases where (*a*) the surface is immediately changed to its new temperature, t'; (*b*) the surface temperature changes at a constant rate; and (*c*) the surface heat transfer coefficient, h, is independent of temperature. Each of these assumptions is a good approximation to certain practical cases, but cannot be arbitrarily applied to any case. No analytical solution is available for the case where cooling is by radiation alone, which is also an important case. Analytical solutions are also available for the case of a composite slab (glaze or enamel).[11] In Fig. 4, temperature distributions for different conditions of surface heat transfer are indicated.

If any arbitrary boundary condition is known or assumed, numerical or graphical methods can be employed to determine the temperature distribution at various time intervals.[9(b), 10] Tables and graphical solutions for a number of common cases also are available in the literature in terms of the nondimensional parameters involved.[12]

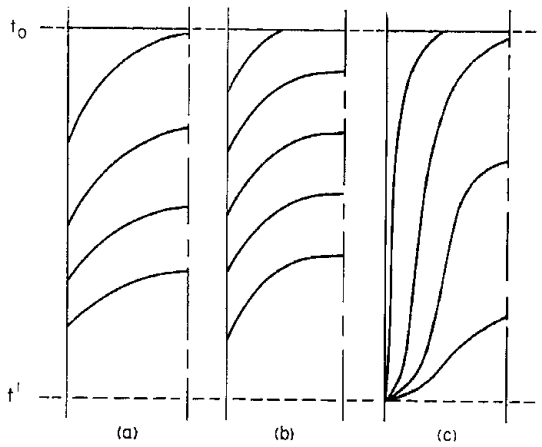

Fig. 4. Temperature decrease through a slab with (*a*) constant surface heat transfer coefficient, (*b*) linear rate surface temperature decrease, and (*c*) immediate cooling of surface from t_0 to t'.

V. Calculation of Resistance to Thermal Stresses[2–5, 13]

The essential method of calculating the resistance to thermal stresses which has been used by all investigators is to determine a temperature distribution under certain conditions and from this to determine the thermal stresses. This method has been applied analytically to various simple shapes and conditions to calculate material property factors. It can also be applied to more complex conditions and shapes by numerical or graphical methods.

A factor of considerable practical interest, and one which

---

[9] (*a*) R. S. Carslaw and J. C. Jaeger, Conduction of Heat in Solids, Oxford University Press, 1947. 386 pp.
(*b*) L. R. Ingersall, O. J. Zobell, and A. C. Ingersoll, Heat Conduction, McGraw-Hill Book Co., Inc., New York, 1948.
(*c*) W. H. McAdams, Heat Transmission, 2d edition, McGraw-Hill Book Co., Inc., New York, 1942. 459 pp.

[10] G. M. Dusinberre, Numerical Analysis of Heat Flow, McGraw-Hill Book Co., Inc., New York, 1949. 227 pp.: *Ceram. Abstr.*, 1952, February, p. 30*d*.

[11] M. L. Anthony, "Temperature Distributions in Composite Slabs Due to Suddenly Activated Plane Heat Source," p. 236; "Temperature Distributions in Slabs With Linear Temperature Rise at One Surface," p. 250, *Proceedings of the General Discussion on Heat Transfer, Inst. Mech. Engrs.*, London (1951).

[12] (*a*) A. J. Ede, "New Form of Chart for Determining Temperatures in Bodies of Regular Shape During Heating or Cooling," *Phil. Mag.*, **36**, 845 (1945).
(*b*) E. D. Williamson and L. H. Adams, "Temperature Distribution in Solids During Heating or Cooling," *Phys. Rev.*, **14**, 99 (1919).
(*c*) H. P. Gurney and J. Lurie, "Charts for Estimating Temperature Distributions in Heating and Cooling Solid Shapes," *J. Ind. Eng. Chem.*, **15** [11] 1170 (1923); *Ceram. Abstr.*, **3** [3] 87 (1924).
(*d*) A. Schack (translated by H. Goldschmidt and E. P. Partridge), Industrial Heat Transfer, John Wiley & Sons, New York, 1933. 371 pp.; *Ceram. Abstr.*, **13** [3] 64 (1934).
(*e*) A. B. Newman, "Heating and Cooling Rectangular and Cylindrical Solids," *Ind. Eng. Chem.*, **28**, 545–48 (1936).
(*f*) A. B. Newman, "Drying of Porous Solids," *Trans. Am. Inst. Chem. Engr.*, **27**, 203, 310 (1931).
(*g*) T. F. Russell, "Some Mathematical Considerations on Heating and Cooling of Steel," First Report of Alloy Steels Research Committee, *Iron & Steel Inst.* (London), *Special Report* No. 14, pp. 149–87 (1936).
(*h*) F. C. W. Olson and O. T. Schultz, "Temperatures in Solids During Heating or Cooling; Tables for Numerical Solution of Heating Equation," *Ind. Eng. Chem.*, **34** [7] 874–77 (1942); *Ceram. Abstr.*, 21 [9] 196 (1942).

[13] (*a*) Bernard Schwartz, "Thermal Stress Failure of Pure Refractory Oxides," *J. Am. Ceram. Soc.*, **35** [12] 325–33 (1952).
(*b*) O. G. C. Dahl, "Temperature and Stress Distributions in Hollow Cylinders," *Trans. Am. Soc. Mech. Eng.*, **46**, 161 (1924).
(*c*) C. H. Kent, "Thermal Stresses in Spheres and Cylinders Produced by Temperature Varying with Time," *Trans. Am. Soc. Mech. Eng.*, **54**, 188 (1932); "Thermal Stresses in Thin-Walled Cylinders," *ibid.*, **53**, 167 (1931).
(*d*) E. M. Baroody, W. H. Duckworth, E. M. Simons, and H. Z. Schofield, "Effect of Shape and Material on Thermal Rupture of Ceramics," AECD-3486, *U. S. Atomic Energy Commission, Natl. Sci. Foundation, Washington, D. C.*, 5–75, May 22, 1951.
(*e*) S. S. Manson, "Behavior of Materials under Conditions of Thermal Stress," N.A.C.A. Tech. Note 2933, July 1953.

(*Footnote 13 continued on page 6*)

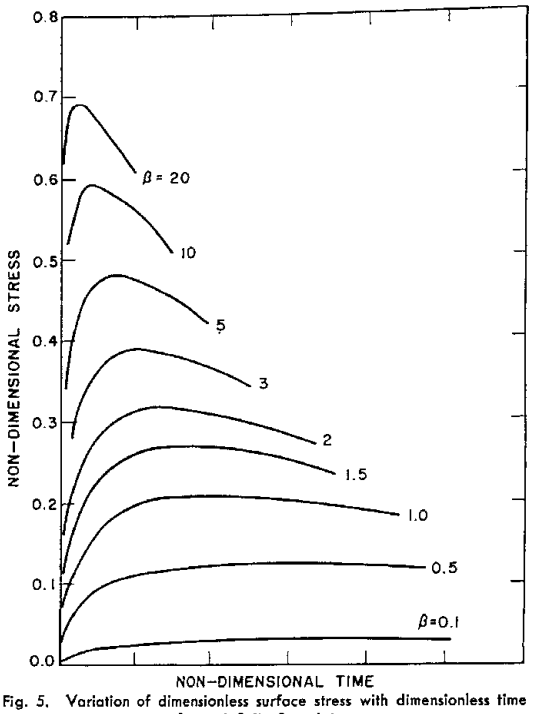

Fig. 5. Variation of dimensionless surface stress with dimensionless time for an infinite flat plate.

serves as a quantitative measure of thermal stress resistance, is the maximum temperature difference required to cause a specified fracture or weakening of a certain shape under specified thermal conditions. For purposes of calculation, the temperature difference causing stresses equal to the breaking strength of the ceramic is employed. Let us consider some typical cases.

(1) Unsteady State (h Infinite)

When the coefficient of heat transfer is so large that the surface originally at t_0 is changed instantly to t', the average temperature of the sample as a whole is at first unchanged from t_0. Consequently, the stress at the surface is (see Table I) for a sphere

$$\sigma = \frac{E\alpha(t_0 - t')}{1 - \mu} \tag{6}$$

$$\sigma_{max} = 1 \tag{7}$$

The dimensionless stress, σ^*_{max}, is the maximum possible, and the temperature difference giving a stress equal to the breaking strength is

$$t_0 - t' = \frac{s_t(1 - \mu)}{E\alpha} \tag{8}$$

On cooling, the surface is in tension and fracture should occur at $\theta = 0$. On heating, the surface stress is compressive, and failure may occur due to shearing stresses which are half the principal stresses:

$$\tau = \frac{E\alpha(t_0 - t')}{2(1 - \mu)} \tag{9}$$

$$t_0 - t' = \frac{2s_s(1 - \mu)}{E\alpha} \tag{10}$$

If this shear stress is insufficient to cause fracture, failure may still occur owing to center tensile stresses. From a well-known solution for the temperature distribution, it can be shown that for a sphere[5]

$$\sigma^*_{max} = 0.386 \tag{11}$$

$$t_0 - t' = \frac{2s_t(1 - \mu)}{0.771E\alpha} \tag{12}$$

The time to fracture is

$$\theta = \frac{0.0574r_m^2}{a} \tag{13}$$

Whether the surface shear or the center tension causes fracture depends on the severity of thermal shock and on the relative shear and center tensile strength.

If a resistance factor in shear or in tension is defined as

$$R = \frac{s_t(1 - \mu)}{E\alpha}; \quad R_s = \frac{s_s(1 - \mu)}{E\alpha} \tag{14}$$

and a shape factor, S, giving the stress dependence on the shape of the specimen, the temperature change which just causes thermal stress fracture can be written as

$$\Delta t_f = R \cdot S \tag{15}$$

The material properties of importance are the breaking stress, Poisson's ratio, modulus of elasticity, and coefficient of expansion.

(2) Unsteady State (h Constant)

This case has received the most attention in the literature and is the simplest condition which approximates many practical cases. By combining known analytical solutions for temperature and stress distribution, thermal stresses can be

(Footnote 13 continued from page 5)

(f) F. J. Bradshaw, "Thermal Stresses in Non-Ductile High-Temperature Materials," Tech. Note MET 100, British RAE, February 1949; "Improvement of Ceramics for Use in Heat Engines," Tech. Note MET 111, British RAE, October 1949.
(g) C. M. Cheng, "Resistance to Thermal Shock," *J. Am. Rocket Soc.*, 21 [6] 147–53 (1951).
(h) W. Buessem, "Ring Test and Its Application to Thermal Shock Problems," O.A.R. Report, Wright-Patterson Air Force Base, Dayton, Ohio (1950).
(i) C. H. Lees, "Thermal Stresses in Solid and in Hollow Circular Cylinders Concentrically Heated," *Proc. Roy. Soc.*, **A101**, 411 (1922); "Thermal Stresses in Spherical Shells Concentrically Heated," *ibid.*, A100, 379 (1921).
(j) B. E. Gatewood, "Thermal Stresses in Long Cylindrical Bodies," *Phil. Mag.*, 32, 282 (1941).
(k) J. C. Jaeger, "Thermal Stresses in Circular Cylinders," *Phil. Mag.*, 36 [257] 418 (1945).
(l) M. J. Lighthill and F. J. Bradshaw, "Thermal Stresses in Turbine Blades," *Phil. Mag.*, 40, 770 (1949).
(m) V. H. Stott, "Thermal Endurance of Glass, I," *J. Soc. Glass Technol.*, 8 [30] 139 (1924); *Ceram. Abstr.*, 3 [10] 281 (1924).
(n) K. Tabata and T. Moriya, "Thermal Endurance of Glass," *J. Am. Ceram. Soc.*, 17 [2] 34–37 (1934).
(o) F. W. Preston, "Theory of Spalling," *J. Am. Ceram. Soc.*, 16 [3] 131–33 (1933); "Spalling of Bricks," *ibid.*, 9 [10] 654–58 (1926).
(p) C. E. Gould and W. M. Hampton, "Thermal Endurance of Glass," *J. Soc. Glass Technol.*, 14 [54] 188–204 (1930); *Ceram. Abstr.*, 9 [10] 830 (1930).
(q) W. G. Lidman and A. R. Bobrowsky, "Correlation of Physical Properties of Ceramic Materials with Resistance to Fracture by Thermal Shock," *Natl. Advisory Comm. Aeronaut. Tech. Note* No. 1918 (1949), 15 pp.; *Ceram. Abstr.*, 1952, January, p. 6*j*.
(r) T. W. Howie, "Spalling of Silica Bricks," *Trans. Brit. Ceram. Soc.*, 45 [2] 45–69 (1946); *Ceram. Abstr.*, 1946, November, p. 195.
(s) R. A. Heindl, "Study of Sagger Clays and Sagger Bodies," *J. Research Natl. Bur. Stand.*, 15 [3] 225–70 (1935); *Ceram. Abstr.*, 15 [1] 23 (1936).
(t) J. F. Hyslop, "Refractories and Thermal Shock," *Trans. Brit. Ceram. Soc.*, 38 [5] 304–12 (1939); *Ceram. Abstr.*, 18 [11] 302 (1939).
(u) A. T. Green and A. J. Dale, "Spalling of Refractory Materials," *Trans. Brit. Ceram. Soc.*, 25 [4] 428–68 (1925); *Ceram. Abstr.*, 6 [10] 445 (1927).

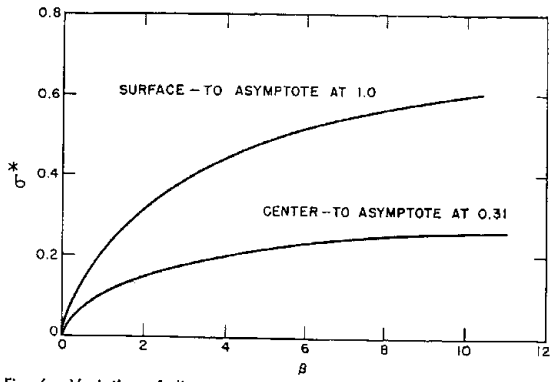

Fig. 6. Variation of dimensionless stress with relative heat transfer rate for an infinite flat plate (footnote 13(f)).

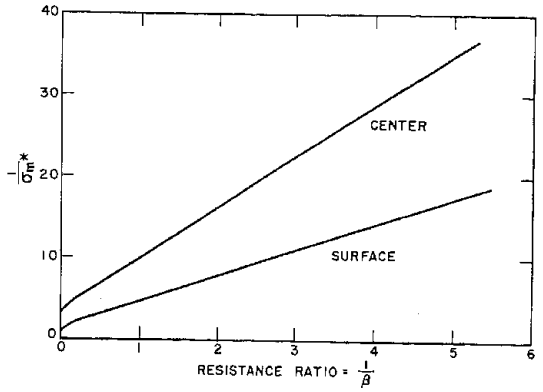

Fig. 8. Variation of $1/\sigma^*_{max}$ with $1/\beta$ for an infinite flat plate (footnote 13(g)).

evaluated as a function of time, coordinates and heat transfer conditions in terms of dimensionless parameters. If stress is plotted as a function of time for different heat transfer conditions, a plot such as Fig. 5 is obtained. Similar curves can be obtained for the center stresses. From the analytical relations or curves such as those shown in Fig. 5, the maximum stress and time to maximum stress can be determined (Figs. 6 through 8).

In view of the complexity of the analytical relations, a number of authors have proposed approximation formulas for the relationship of maximum stress and rate of heat transfer. For relatively low values of β (which are of major importance for gas convection and radiation cooling) the following relationships have been suggested for the surface stress:

Bradshaw:[13(f)]

$$\frac{1}{\sigma^*_{max}} \cong \frac{4}{\beta} \tag{16}$$

Buessem:[13(h)]

$$\frac{1}{\sigma^*_{max}} \cong 1 + \frac{4}{\beta} \tag{17}$$

Cheng:[13(g)]

$$\frac{1}{\sigma^*_{max}} \cong \frac{3}{\beta} \tag{18}$$

Manson:[13(e)]

$$\frac{1}{\sigma^*_{max}} \cong \frac{3.25}{\beta} \tag{19}$$

In this condition, taking the simplest relationship, that σ^*_{max} = (constant) β, the thermal stress resistance can be evaluated as

$$\frac{s_t(1-\mu)}{E\alpha(t_0 - t')} = (\text{constant})\,\frac{r_m h}{k} \tag{20}$$

$$(t_0 - t') = \frac{k s_t(1-\mu)}{E\alpha}\left[\frac{1}{(\text{constant})\ (r_m h)}\right] \tag{21}$$

Defining a second thermal stress resistance factor

$$R' = \frac{k s_t(1-\mu)}{E\alpha} \tag{22}$$

and including the constant from equation (21) in the shape factor

$$\Delta t_f = R' \cdot S \cdot \frac{1}{h} \tag{23}$$

The thermal stress resistance factor for this case includes the thermal conductivity, k, in addition to μ, E, α, and s_t.

Over a wider range of heat transfer rates, analytical solutions have been obtained by Cheng and various approximations have been suggested. Approximation formulas have been suggested by Buessem and Manson. As the rate of heat transfer increases, the problem degrades into the case of infinite h, which was treated previously.

Another problem is the temperature at which to evaluate

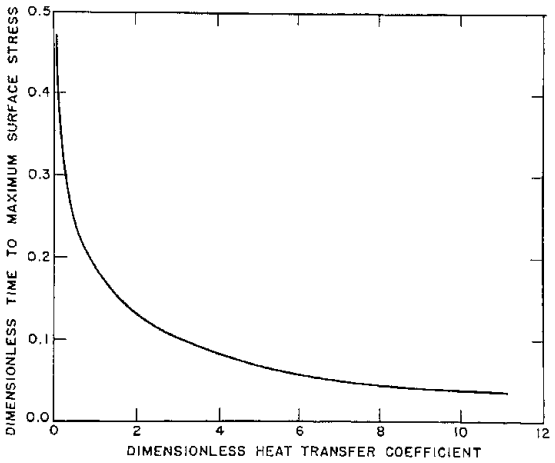

Fig. 7. Variation of dimensionless time to maximum surface stress with relative heat transfer rate.

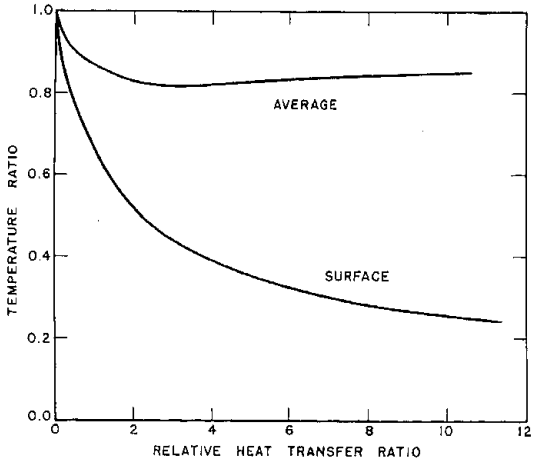

Fig. 9. Relative average and surface temperatures at time of maximum stress under various heat transfer ratios (footnote 13(e)).

the material properties involved. In Fig. 9, the average and surface temperatures at time of maximum stress are quite high, particularly for the low values of β. Consequently, values of temperature-dependent properties should usually be selected at a relative temperature of 0.8 to 0.9 rather than at a completely arbitrary mean temperature.

This analysis of thermal resistance indicates that at least two thermal resistance factors must be considered (as has been emphasized by Buessem, Bradshaw, and others). For high rates of heat transfer, the thermal resistance is proportional to $s_t(1-\mu)/E\alpha$. At low rates of heat transfer, the thermal resistance is proportional to $ks_t(1-\mu)/E\alpha$. No single thermal resistance factor can adequately characterize a material for various conditions.

(3) Steady State

Steady nonlinear temperature gradients give rise to thermal stresses which may be sufficient to cause thermal stress failure. The steady state temperature distribution depends on the thermal conductivity and on the rate of heat flow per unit area,

$$\frac{dt}{dx} = -\frac{q}{kA} \tag{24}$$

For any given sample, if S is a shape factor and Δt is the overall temperature difference,

$$q = -kS\,\Delta t \tag{25}$$

and the conditions can be uniquely defined by specifying either the heat flow or the temperature difference. For an infinite hollow cylinder with an interior heat source, the temperature distribution is logarithmic and the tensile stress at the outer surface is given by

$$\sigma = \frac{E\alpha\,\Delta t}{(1-\mu)} \cdot \frac{\left(1 - \frac{2r_1^2}{r_2 - r_1}\ln\frac{r_2}{r_1}\right)}{2\ln\frac{r_2}{r_1}} \tag{26}$$

and the maximum temperature difference is

$$\Delta t_f = \frac{s_t(1-\mu)}{E\alpha} \cdot \frac{2\ln\frac{r_2}{r_1}}{1 - \frac{2r_1^2}{r_2^2 - r_1^2}\ln\frac{r_2}{r_1}} = R\cdot S \tag{27}$$

for radial heat flow,

$$q = \frac{2\pi k\,\Delta t}{\ln\frac{r_2}{r_1}}$$

and at fracture,

$$q_{\max} = \frac{ks_t(1-\mu)}{E\alpha} \cdot \frac{4\pi}{1 - \frac{2r_1^2}{r_2^2 - r_1^2}\ln\frac{r_2}{r_1}} = R'\cdot S \tag{28}$$

Since the possible heat flow at steady state is usually the factor of interest, the resistance factor, R' (including the thermal conductivity), is the one of interest. For some applications, the temperature difference may be of more interest, and in this case the factor R (excluding thermal conductivity) is of importance.

(4) Constant Rate of Heating or Cooling

When a furnace is heated or cooled at a constant rate, the effective value of h changes with temperature. In this case, the temperature gradients and stress depend on the rate of cooling, and if the constant rate of surface temperature change is ϕ°C. per second, the stress for a plane slab is

$$\sigma = \frac{E\alpha}{(1-\mu)} \cdot \frac{\phi r_m^2}{3a} \text{ (surface)} \tag{29}$$

$$\sigma = \frac{E\alpha}{(1-\mu)} \cdot \frac{\phi r_m^2}{6a} \text{ (center)} \tag{30}$$

The maximum rate of temperature change without fracture, if S is a shape and size factor, is

$$\phi_{\max} = \frac{s_t(1-\mu)a}{E\alpha}\cdot S = R''\cdot S \tag{31}$$

Consequently, under these conditions a third resistance factor involving material properties must be considered, which includes the thermal diffusivity.

(5) Properties Determining Thermal Stress Resistance

Consideration of three specific cases of heat-transfer conditions leads to three "resistance" factors which apply to different conditions. Other specific cases might require additional material factors. For example, under conditions of cooling by radiation, the emissivity of the surface would affect the rate of cooling, and consequently the thermal stresses. In addition, the equivalent equations for shear may apply to some cases of heating and a shape or size factor must be employed for applications to specific bodies. Consequently, it is not possible to list a single factor called "resistance to thermal stresses" as a material property such as density or coefficient of expansion. Instead, the conditions and specimen shape employed may markedly change the results found. The properties which affect thermal stress resistance are elasticity, strength, coefficient of expansion, Poisson's ratio, and, in some cases, thermal conductivity, diffusivity, or emissivity.

It should be emphasized that the results here apply exactly only to a homogeneous isotropic body whose physical properties are substantially independent of temperature. Deviations should be expected for materials with sharply temperature-dependent properties, or nonhomogeneous materials such as refractory brick containing significant amounts of grog or metal-ceramic composites.

(6) Thermal Spalling

Thus far only the stress required to initiate a fracture has been considered. An additional problem is whether propagation of the fracture with consequent spalling will follow. Once a crack begins, the stress distribution is drastically altered and mathematical analysis is not feasible.

Griffith's criterion for crack propagation[14] is that the strain energy released must be equal to, or greater than, the surface energy of the new surfaces formed. Consequently, it can be expected that the spall formed will release the maximum strain energy.[13(o)] For an infinite slab with temperature distributions such as shown in Fig. 4, the strain energy in a unit volume is given by

$$u = \frac{\sigma^2(1-\mu)}{E} \tag{32}$$

and it would be expected that the depth of the spall should be proportional to $E/(1-\mu)\sigma^2$. Since the residual temperature gradient in the spalled piece will be nearly linear, essentially all its strain energy will be removed on spalling. Consideration of strain energy as a criterion of spalling leads to the same stress resistance factors as does consideration of the stresses required to initiate fracture. If the necessary depth of spall is large enough, the initial crack may not propagate to this depth and surface checking without spalling can result.

Calculation of strain energy release as a function of time and depth is not difficult. The effect of cracks altering the stress distribution and the essentially similar results from calculation of maximum stress make the general usefulness of quantitative strain energy calculations questionable.

---

[14] A. A. Griffith, "Phenomena of Rupture and Flow in Solids," *Phil. Trans. Roy. Soc.*, **A221**, 163 (1920).

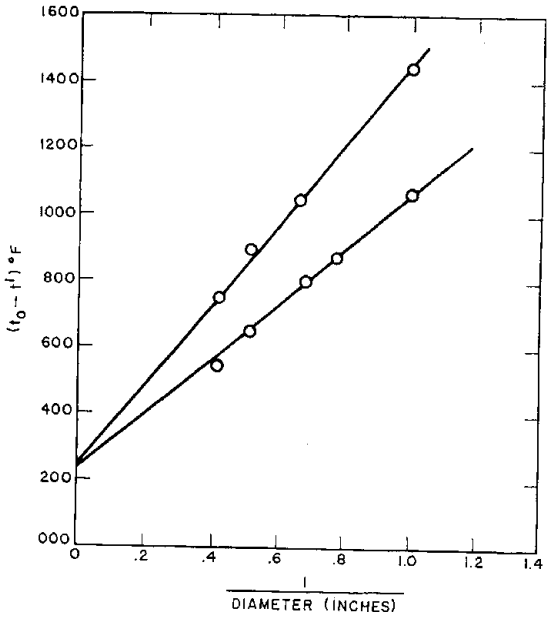

Fig. 10. Effect of specimen size on thermal stress resistance of steatite quenched by air or water blast (footnote 13(e)).

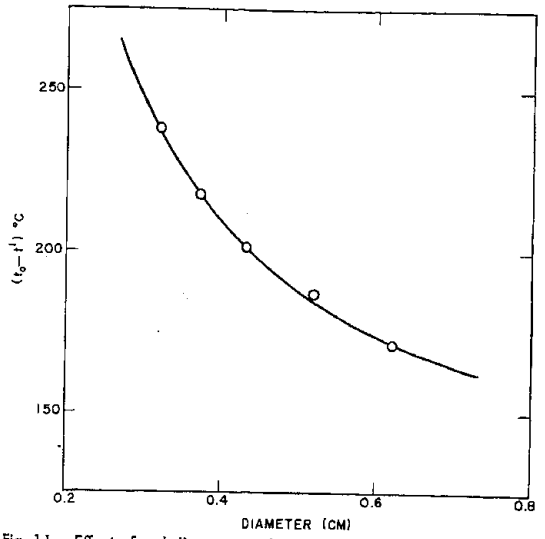

Fig. 11. Effect of rod diameter on thermal stress resistance of glass rods quenched in water bath (footnote 13(n)).

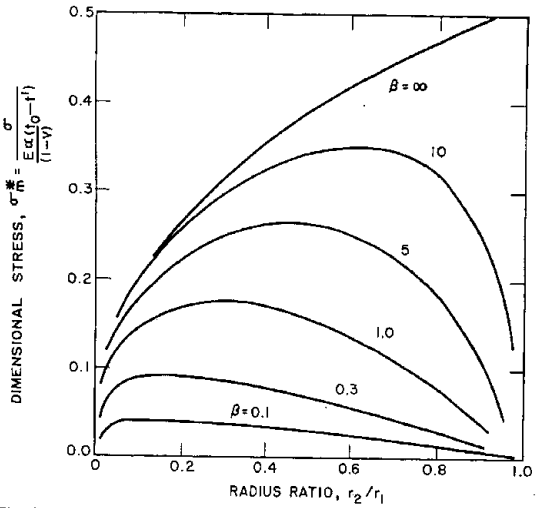

Fig. 12. Variation of surface stress (r_2) for hollow cylinder where outer radius is maintained at constant temperature, t' (footnote 13(f)).

All the previous calculations of resistance to thermal stress have assumed a homogeneous body and have determined when the maximum thermal stress will be equal to the breaking strength. In practice, however, particularly under conditions of thermal shock tests, the minimum thermal stress required to cause surface checking will not fracture a normal ceramic body. In a quenching test, the maximum stress at the surface decreases rapidly and is much higher than the stress at the interior points so that the crack does not continue to fracture. In subsequent tests, these surface cracks act as stress-concentrators and the actual stress is probably too complex to calculate. We would expect that additional thermal cycles of the same magnitude as required to initiate surface cracks would lead to eventual fracture and spalling, but this may not always be true.

As far as we are aware, the only measurements reported for the depth of thermal stress fractures are those of Howie for silica brick.[13(r)] His data are in good agreement with results predicted from considerations of maximum strain energy.

VI. Factors Affecting Thermal Stress Resistance

Although the general theory of thermal stress resistance which we have outlined seems quite satisfactory, it depends on various material properties and on simplifying assumptions. Differences in material properties and deviations from the simplifying assumptions must be considered in any practical applications.

Table II. Temperature Differences Between Surface and Center of Various Shapes Cooled at a Constant Rate $\phi = dt/d\theta$

Shape	$t_c - t_s$
Infinite plate, half thickness = r_m	$0.50\ \frac{\phi r_m^2}{a}$
Infinite cylinder, radius = r_m	$0.25\ \frac{\phi r_m^2}{a}$
Cylinder, half length = radius = r_m	$0.201\ \frac{\phi r_m^2}{a}$
Cube, half thickness = r_m	$0.221\ \frac{\phi r_m^2}{a}$

(1) Specimen Size and Shape[13(c)–(h)(n),15]

Neglecting end effects for a moment, the major effect of increased size is to increase the nondimensional heat-transfer parameter, $\beta = r_m h/k$. When the specimen size is sufficiently large, conditions approach the case where the surface temperature is altered without changing the mean body temperature, the thermal stress resistance is substantially inde-

[15] (*a*) O. H. Clark, "Resistance of Glass to Thermal Stresses," *J. Am. Ceram. Soc.*, **29** [5] 133–38 (1946).
(*b*) J. B. Murgatroyd, "Effect of Shape on Thermal Endurance of Glass Rods," *J. Soc. Glass Technol.*, **27** [119] 5–17T (1943); *Ceram. Abstr.*, **22** [10] 170 (1943); "Effect of Shape on Thermal Endurance of Cylindrical Glass Containers," *J. Soc. Glass Technol.*, **27** [121] 77–93T (1943); *Ceram. Abstr.*, **23** [1] 8 (1944).
(*c*) M. D. Karkhanavala and S. R. Scholes, "Relation Between Diameter and Thermal Endurance of Glass Rods," *J. Soc. Glass Technol.*, **35** [167] 289–303T (1951); *Ceram. Abstr.*, **1952**, September, p. 158*i*.

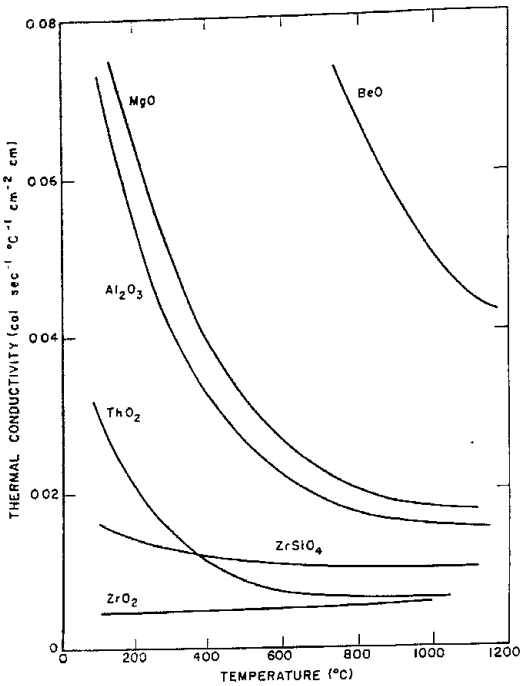

Fig. 13. Thermal conductivity of some ceramic materials.

pendent of h and k, and $\sigma^*_{max} = 1$. Conversely, for very small specimens, even very high rates of cooling will not approach the case where $\sigma^*_{max} = 1$. For moderate rates of temperature change, the thermal stress is approximately proportional to $r_m h/k$, and consequently thermal stress resistance is inversely proportional to specimen dimensions. Data of Manson[13(e)] for steatite (Fig. 10) follow this relationship. For very high rates of cooling, the relationship is more complex. Data for glass rods quenched in water[13(a)] indicate that the size effect becomes important for rod diameters below 6 to 8 mm. (Fig. 11). For the steady state, the temperature drop for a given heat flow is directly proportional to wall thickness and increased thermal stresses occur. If, however, the temperature drop (rather than heat flow) is maintained constant, no stress increase results.

In addition to the size factor, the shape is also of importance, as has been indicated by the inclusion of a general shape factor, S, in the equations for thermal stress resistance. The effect of shape for stress calculation is shown in Table I. A pronounced case is unsteady-state heat flow in hollow cylinders, as occurs in rocket nozzles. The nondimensional stress for heating the interior of a hollow cylinder with different radius ratios is shown in Fig. 12, for various rates of heat transfer in the limiting case after an infinite time.[13(f)] The maxima are roughly on a line where $\sigma^* = {}^1/_2 r_1/r_2$ (where $r_1 < r_2$). Similarly, the maximum temperature differences for a few shapes cooled at a constant rate of temperature change are shown in Table II. These variations give rise to considerable changes in thermal stresses.

Another important effect which is more difficult to assess is the presence of edges and corners in finite slabs, cylinders, wedges, and other shapes. For simple shapes, these can be estimated from elastic theory. Kent[13(c)] has estimated the stresses for long thin-walled cylinders and finds an increase of about 30% in tangential stress at the ends as compared to an infinite cylinder. Baroody *et al.*[13(d)] have made some experimental measurements for this case. Lighthill and Bradshaw[13(f)] considered the stresses in a wedge, and found that, on

Table III. Values of Surface Heat-Transfer Coefficient, h

Conditions	h (B.t.u. hr.$^{-1}$ °F.$^{-1}$ ft.$^{-2}$)	h (cal. sec.$^{-1}$ °C.$^{-1}$ cm.$^{-2}$)
Air flow past cylinder:		
Flow rate 60 lb. sec.$^{-1}$ ft.$^{-2}$	190	0.026
Flow rate 25 lb. sec.$^{-1}$ ft.$^{-2}$	90	.012
Flow rate 2.5 lb. sec.$^{-1}$ ft.$^{-2}$	20	.0027
Flow rate 0.025 lb. sec.$^{-1}$ ft.$^{-2}$	2	.00027
Radiation to 0°C. from 1000°C.	26.0	.0035
Radiation to 0°C. from 500°C.	7.0	.00095
Water quenching	1000–10,000	.1–1.0
Jet turbine blades	35–150	.005–0.02 (Cheng, Bradshaw)

heating, the largest initial stresses were at the edge, but the maximum stress occurred at the thickest portion on both heating and cooling. Norton[4] studied the stresses developed in brick shapes with the use of polarized light. In general, experimental measurements of this type are probably the best method for studying complex shapes. Many cases, such as built-up walls, or cylinders and slabs where the ends are not maintained at the same temperature difference as the central portion, can be satisfactorily treated as infinite bodies.

(2) Heat-Flow Properties[0,10,11,13(e)–(h),16]

The rate of heating or cooling is an important factor in the development of thermal stresses and is affected both by the conditions imposed and by the physical properties of the material concerned.

Measurements of the heat transfer coefficient, h, which are available are largely for steady-state heat exchange. Few measurements under transient conditions are available. Some values which seem representative are given in Table III. As far as the author is aware, no measuremnts are available for conditions such as occur in jet engines and other current applications. Measurements at steady state are not directly applicable since surface heat transfer coefficients vary considerably with the film temperature when heat transfer is mainly by convection. Measurements of β can be obtained by determining the rate of change of temperature of any point, or the simultaneous temperature of several points. By analytical equations, or more simply by comparison with plotted or tabulated solutions, relative values of a and β can be determined for the specific conditions employed. If k and c_p are known, the surface heat transfer coefficient, h, can be determined. Materials of known and constant (with temperature) k and c_p should be employed.

The assumption that h remains constant, which is taken for most thermal stress calculations, is only an approximation for most practical cases, and can be expected to hold closely only

---

[16] (*a*) W. D. Kingery, J. Francl, R. L. Coble, and T. Vasilos, "Thermal Conductivity: X, Data for Several Pure Oxide Materials Corrected to Zero Porosity," *J. Am. Ceram. Soc.*, **37** [2, Part II], 107–10 (1954).

(*b*) M. C. Booze and S. M. Phelps, "Study of Factors Involved in Spalling of Fire-Clay Refractories with Some Notes on Load and Reheating Tests and Effect of Grind on Shrinkage," *J. Am. Ceram. Soc.*, **8** [6] 361–82 (1925).

(*c*) A. R. Bobrowsky, "Applicability of Ceramics and Ceramals as Turbine-Blade Materials for the Newer Aircraft Power Plants," *Trans. Am. Soc. Mech. Engrs.*, **71** [6] 621–29 (1949); *Ceram. Abstr.*, **1951**, February, p. 28*f*.

(*d*) F. G. Code Holland, "Ceramics and Glass: I, Use of Ceramic Coatings in Gas Turbine Combination Chambers," *Selected Govt. Research Repts.*, 10, 1–7 (1952); *Ceram. Abstr.*, **1953**, April, 56*j*.

(*e*) D. G. Moore, S. G. Benner, and W. N. Harrison, "Studies of High-Temperature Protection of a Titanium-Carbide Ceramal by Chromium-Type Ceramic-Metal Coatings," *Natl. Advisory Comm. Aeronautics Tech. Note* No. 2386 (1951), 26 pp.

(*f*) F. H. Norton, Refractories, 3d edition, McGraw-Hill Book Co., Inc., New York, 1951. 782 pp.

Table IV. Thermal Conductivity of Ceramic Materials*

Material	k (cal. sec.$^{-1}$ °C.$^{-1}$ cm.$^{-2}$ cm.) 100°C.	400°C.	1000°C.
Al_2O_3	0.072	0.031	0.015
BeO	.525	.222	.049
Graphite	.426	.268	.149
MgO	.086	.039	.017
Mullite	.015	.011	.010
Spinel	.036	.024	.014
ThO_2	.025	.014	.008
Zircon	(.016)	.012	.010
ZrO_2 (stabilized)	.0047	.0049	.0055
Fused quartz	.0038	.0045	
Soda-lime-silica glass	.0040	.0046	
TiC	.060	.032	.014
Porcelain	.0041	.0042	.0045
Fire-clay refractory	.0027	.0029	.0037
TiC cermet	.083	(.04)	(.02)

* Data for crystalline materials are for theoretical density. Values in parentheses are estimated.

Table V. Mean Coefficient of Linear Expansion for Some Ceramic Materials (30° to 1000°C.)

Material	$\alpha \times 10^{-6}$ (°C.$^{-1}$)
Al_2O_3	8.8
BeO	9.0
MgO	13.5
Mullite	5.3
Spinel	7.6
ThO_2	9.2
Zircon	4.2
ZrO_2 (stabilized)	10.0
Fused quartz	0.5
Soda-lime-silica glass	9.0
TiC	7.4
Porcelain	6.0
Fire-clay refractory	5.5
TiC cermet	9.0

when $(t_0 - t')$ is small. This is a reasonable approximation for glasses and ceramic bodies having relatively poor thermal stress resistance; it is probably poor for the better materials and for more rigorous applications such as jet engines and refractory furnaces. Other important cases are where the surface temperature changes linearly (as in the controlled heating or cooling of a furnace, or as an approximation to more complex conditions), and where the heat transfer is proportional to $(t_0^4 - t'^4)$ as in radiant heat transfer.

Another factor which complicates the picture and has been essentially neglected in analytical calculations is changes in c_p and k with temperature. A sharp change in heat capacity changes the temperature distribution and, consequently, the stresses considerably in the transient state. Although such changes are not usual in ceramic materials, a sharp decrease in the thermal conductivity of dense crystalline ceramics does normally occur as shown in Fig. 13. BeO changes by a factor of ten between 100° and 1000°C., whereas MgO and Al_2O_3 change by a factor of six. Data for the thermal conductivity of a number of ceramic materials are given in Table IV. It might be noted that many measurements of conductivity given in the literature are not satisfactory. In addition, the changes in conductivity with temperature make results calculated from room-temperature values most doubtful. At room temperature, the variation between materials amounts to a factor of 100; at 1000°C. the variation is decreased to a factor of 10. For glasses and fire-clay refractories, the variation between roughly similar compositions is not large, and conductivity is not such an important factor. For pure crystalline materials the porosity and purity become quite important. A few per cent silica in an alumina body may decrease the conductivity to half the value for pure alumina. Similar results are found for a few per cent solid solution.

For stresses arising on cooling, a high thermal conductivity is always desirable. On heating for short time periods, a high conductivity leads to decreased surface compressive and shear stresses, but gives a somewhat increased center tensile stress at short times. If failure occurs due to a center tensile failure and times are short, a low conductivity may be advantageous depending on the time and rate of heating, on relative shear and tensile strengths, and on the relative thermal conductivities. No specific general relations or experimental data are available.

The presence of a glaze or ceramic coating on a surface acts essentially as an additional thermal resistance which decreases the effective cooling or heating rate at the interface. Consequently, even if the coating fractures, it may decrease body stresses by decreasing the intensity of thermal shock. This effect will be additive with any stresses due to the differential expansion of coating and body.

(3) Coefficient of Thermal Expansion[2,3,4,8(b),13(r)–(u),16(f),17]

For any given temperature distribution, the thermal stresses are directly related to the thermal expansion. Compared with other properties, the expansion coefficient remains relatively constant over the temperature range of interest for homogeneous bodies unless a magnetic or polymorphic transformation occurs (as in silica, zirconia, and some other materials). Consequently, an average expansion coefficient is usually satisfactory. Values for a number of materials are given in Table V. Measurements by well-known methods are not difficult. The expansion coefficient varies considerably for different materials and will be the major factor affecting thermal stresses in most glasses and many refractory and whiteware compositions. Some materials, such as Stupalith, aluminum titanate, and fused silica, have extremely low coefficients of expansion (but may be unsatisfactory for other reasons, such as low strength or poor creep resistance).

For cases where the expansion coefficient changes with temperature (transformation, as for α-β cristobalite) or through the specimen (as for a glazed body), thermal stresses can be determined by taking the product, αt, as the temperature variable. Then, for example, for the surface stress

[17] (*a*) J. H. McKee and A. M. Adams, "Physical Properties of Extruded and Slip-Cast Zircon with Particular Reference to Thermal Shock Resistance," *Trans. Brit. Ceram. Soc.*, 49, 386–407 (1950).
(*b*) R. E. Stark and B. H. Dilks, Jr., "New Lithium Ceramics," *Materials and Methods*, 35 [1] 98–9 (1952).
(*c*) K. Endell, "Gegen Temperatur änderungen unempfindliche Magnesitsteine" (Magnesite Brick Not Affected By Temperature Changes), *Stahl u. Eisen*, 52 [31] 759–63 (1932); *Ceram. Abstr.*, 11 [12] 616 (1932).
(*d*) R. A. Heindl, "Thermal Spalling of Fire-Clay Brick in Relation to Young's Modulus of Elasticity, Thermal Expansion, and Strength," *Am. Refractories Inst. Tech. Bull.*, 58 (May 1935); *Ceram. Abstr.*, 15 [7] 210 (1936).
(*e*) J. J. Gangler, "Some Physical Properties of Eight Refractory Oxides and Carbides," *J. Am. Ceram. Soc.*, 33 [12] 367–74 (1950).
(*f*) H. R. Goodrich, "Spalling and Loss of Compressive Strength of Fire Brick," *J. Am. Ceram. Soc.*, 10 [10] 784–94 (1927).

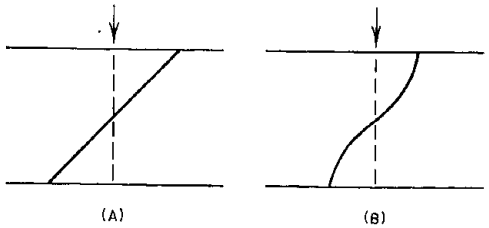

Fig. 14. Deviation from Hooke's law causes actual stress distribution (b) to differ from assumed distribution (a).

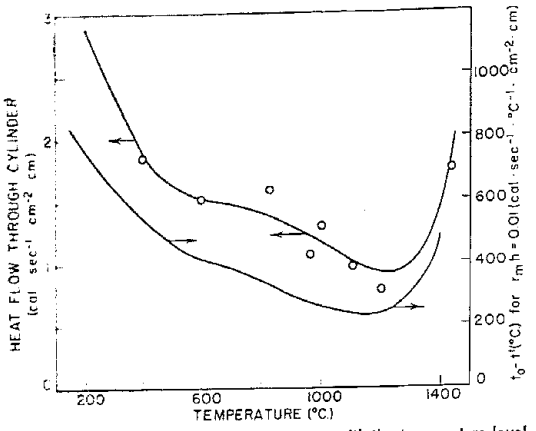

Fig. 15. Variation in thermal stress resistance with the temperature level of testing (data from Schwartz, footnote 13(a)).

$$\sigma = \frac{E}{1-\mu}\,(l_0{}^{\alpha}t_s s - t_0{}^{\alpha}t_a{}'a) \qquad (33)$$

In the case of a glaze or enamel, residual stresses due to unequal cooling contraction of glaze and body will be additive with thermal stresses. These have been considered in equations (1) and (2). These stresses, together with thermal stresses calculated from the temperature distribution and from equation (33), provide a reasonable basis for studying the thermal stress resistance of glazed bodies.

(4) Elastic Properties[13(a)(g)(e)(w),16(f),17,18]

In the analysis of resistance to thermal stresses, we assumed that the material was perfectly elastic (no plastic or viscous flow) and obeyed Hooke's law up to the breaking stress. For brittle ceramic materials, these assumptions are quite good at low temperatures, and E is almost independent of t at low temperatures. As the temperature increases, there is a decrease in E due to grain-boundary relaxation, and at still higher temperatures, plastic or viscous flow takes place. Measurement of E is possible either in tension or in a bend test. At higher temperatures, where some plastic flow can occur, the stress distribution is different than that assumed as shown in Fig. 14, and a low value of E results. However, in thermal stress calculations, we also assume that Hooke's law applies for stresses similar to those shown in Fig. 15. Consequently, the best approximation for elevated temperatures is probably to employ E measured in bend tests, even though this may not be a true elastic constant.

In tests of commercial refractories, Heindl, Endell, and Norton have all found that the elastic deformation is an important factor which varies considerably between various materials. Experimental data for thermal spalling show a direct relation between thermal endurance and 1/extensibility ($= E/s_t$ where the extensibility $= s_t/E$ or the strain to fracture).

Poisson's ratio, μ, which enters into the equation for thermal stress resistance, is relatively constant between materials (varying between 0.18 and 0.35) and with temperature. At higher temperatures, the measured value of μ decreases. The only case for which a very marked variation of μ is found is for anisometric materials, such as impregnated glass fiber compositions. This may become important if oriented ceramic compositions become available. Some typical values of E and μ for ceramic materials are given in Table VI.

Table VI. Values of E and μ for Ceramic Materials

Material	E, lb./sq. in. × 10^6			μ
	20°C.	400°C.	1000°C.	20°C.
Al_2O_3	51.0	49.2	45.0	0.20
BeO	44.	40.	30.	0.38
MgO	30.5	30.0	21.0	0.36
Mullite	21.0	19.5	11.0	0.30*
Spinel	34.5	34.3	30.4	0.31
ThO_2	21. (39.5)	19.	17.	0.17
Zircon	13.6 (30)	13.5	12.7	0.35
ZrO_2 (stabilized)	21.5 (26)	20.1	19.9	0.29
Fused quartz	10.5	10.9		0.15
Soda-lime-silica glass	9.5	9.5		0.20
TiC	45.	45.	40*	0.30*
Porcelain	10.	9.	6.	0.30*
Fire-clay refractory	2.5	2.3	0.5	0.30*
TiC cermet	60.	60.	55.	0.30*

* Estimated

Poisson's ratio, μ, which enters into the equation for thermal stress resistance, is relatively constant between materials (varying between 0.18 and 0.35) and with temperature. At higher temperatures, the measured value of μ decreases. The only case for which a very marked variation of μ is found is for anisometric materials, such as impregnated glass fiber compositions. This may become important if oriented ceramic compositions become available. Some typical values of E and μ for ceramic materials are given in Table VI.

The effect of ductility or plastic flow at elevated temperatures is known to be considerable. Numerous experiments have shown that at temperatures where ceramic materials show plastic or viscous flow, thermal stress failure is negligible. The stress resistance of some cermet bodies may be due in part to the development of some ductility at use temperatures.

(5) Strength[13(a)(g)(e)(w),14,15(a),16(f),17,18,19]

On cooling, the most dangerous thermal stresses are tensile; on heating, either shear or tensile stresses may be most dangerous. Since the compressive strength of ceramics is four to eight times the tensile strength, failure from compressive stresses is unimportant. Tensile strength may be measured in tensile tests, in bending tests, or in torsional tests. In tensile tests, unless extreme precautions are taken, failure may occur due to stress concentration in the grips or with additive stresses due to poor specimen alignment, which is most difficult to avoid for brittle ceramics. In bending and torsion tests (in which ceramic materials always fail in tension), the actual and theoretical stress distributions differ from materials which do not follow Hooke's law, as in Fig. 14. Consequently, the measured strengths are higher than actual strengths. In addition, the different volumes of specimen under stress may affect strength due to the probability of a flaw being present in a greater volume. These factors combine to give higher values to tensile strength measured in torsion and bend tests than that measured in tensile tests (variations from 1:1 to 3:1 are found). For thermal stress applications, the greater similarity of stress distribution in bending and torsion tests to that occurring due to temperature gradients, and the relatively greater freedom from stress concentration and alignment effects make these methods of measurement preferable.

Other complicating effects are the possibility of delayed

[18] (a) E. Endell and F. Angeleri, "Torsion Properties of Stakolumite (Flexible Brazilian Sandstone), Crummendorf Quartzschist, and Some Sandstones," *Ber. deut. Keram. Ges.*, 19, 359 (1938).
(b) R. A. Heindl and L. E. Mong, "Young's Modulus of Elasticity, Strength, and Extensibility of Refractories in Tension," *J. Research Natl. Bur. Stand.*, 17 [3] 463–82 (1936); RP 923; *Ceram. Abstr.*, 16 [1] 24 (1937).
(c) R. A. Heindl and W. L. Pendergast, "Deformation and Young's Modulus of Fire-Clay Brick in Flexure at 1220°C.," *J. Research Natl. Bur. Stand.*, 19, 353–66 (1937); *Ceram. Abstr.*, 17 [1] 19 (1938).
(d) R. A. Heindl and W. L. Pendergast, "Progress Report on Investigation of Fire-Clay Brick and Clays Used in Their Preparation," *J. Am. Ceram. Soc.*, 12 [10] 640–75 (1929).

[19] (a) H. S. Roberts, "Cooling of Optical Glass Melts," *J. Am. Ceram. Soc.*, 2 [7] 543–63 (1919).
(b) F. W. Preston, "Study of Rupture of Glass," *J. Soc. Glass Technol.*, 10 [39] 234–69 (1926); *Ceram. Abstr.*, 13 [3] 57 (1934).
(c) J. B. Murgatroyd, "Strength of Glass," *J. Soc. Glass Technol.*, 17 [67] 260 (1933); *Ceram. Abstr.*, 13 [3] 57 (1934).

fracture, which has been thoroughly investigated for glasses, but not for other ceramics, and the effects of surfaces. Breaking strength of glasses depends on the time of loading due to atmospheric contamination of the fracture surfaces. There has been some suggestion that time of loading may also affect dense Al_2O_3, but the effect has not been unequivocably demonstrated. For ceramic bodies containing a considerable amount of glassy phase, the effect may be considerable. The strength for stresses at the interior of a specimen may be considerably higher than for the stresses at a surface. Consequently, the quantitative application of measured tensile strengths to center stresses is questionable.

Measurements of true shear strengths are difficult and, in general, not available. Failure in compressive tests always occurs in shear, so that the shear strength may be, in general, taken as two to four times the tensile strength. As far as the author is aware, it is always equal to or greater than the tensile strength for ceramic materials.

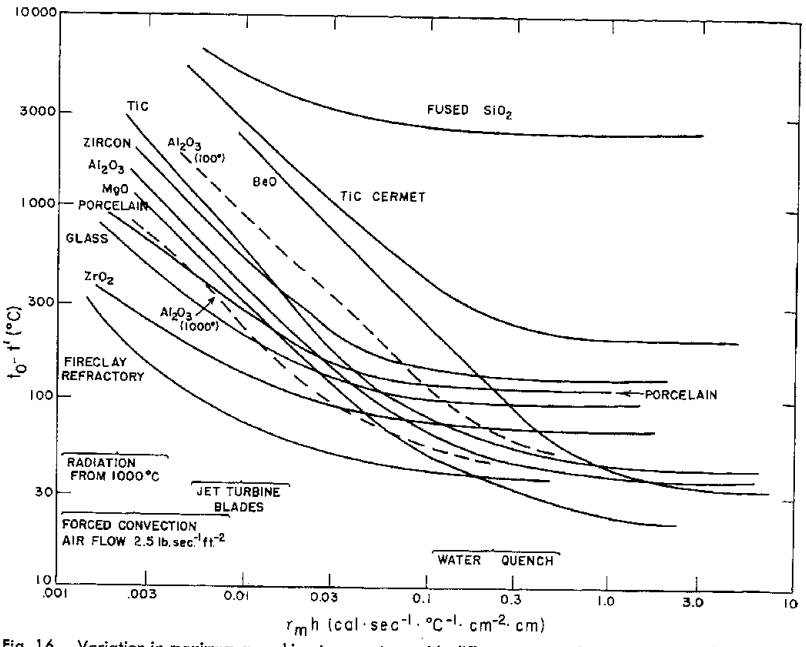

Fig. 16. Variation in maximum quenching temperature with different rates of heat transfer. (Calculated from material properties at 400°C. Dashed curves for Al_2O_3 calculated from material properties at 100° and 1000°C.).

In general, the highest strength values are found for dense crystalline ceramics and some of the cermet materials. Strength of fire-clay refractories varies considerably, being increased by harder firing and lower porosity, whereas the tensile strength of usual glass compositions does not vary widely with composition, but may be increased considerably by suitable surface treatment. In general, materials of high strength also have high values of elastic moduli, so that firing to increase strength may not improve the ratio s_t/E which is of importance for thermal stress resistance. Values of ultimate strength for some ceramic materials are given in Table VII. As seen there, the variation between materials is considerable.

In some cases, improvements in strengths for thermal stress applications have been obtained by prestressing. The normal thermal shock resistance of tempered glass is considerably greater than annealed glass due to compressive stresses developed on the surface. The maximum quenching temperature of one glass was decreased from 145° to 120°C. by annealing. On heating, however, where compressive stresses arise, the maximum Δt_f was *increased* from 426° to 477°C. by annealing.[20] Development of prestressing by glazes has been considered previously. A study of prestressing by flame spraying a metal coating on ceramics gave encouraging results in certain cases.[21] For any of these prestressing techniques, the possibility of stress relaxation in use must be considered.

In actual designs, the stress distribution may differ considerably from that calculated, giving lower effective strengths due to stress concentration or restraints in the design or to the effects of erosion or corrosion in use.

(6) Combined Effect of Material Properties

The resistance of materials to thermal stresses generally depends on the factors $[s_t(1-\mu)/E\alpha]$ and $[ks_t(1-\mu)/E\alpha]$ and no one material property or condition can be taken as a uniform criterion. In general, composition changes which give rise to high strengths also increase E, so that the ratio s_t/E should be considered instead of either factor alone. The "extensibility" or maximum strain to fracture may vary considerably, and individual factors affecting it have not been analyzed separately. In general, it is low for underfired and overfired brick, but factors such as crystal development, glass formation, and porosity have not been separately investigated. Thermal conductivity and the coefficient of expansion vary considerably for different materials and have a considerable effect on thermal stress resistance. In particular, the almost direct relationship between silica content and spalling resistance of firebrick is due to increased expansion.

The temperature level of thermal stress tests may have a considerable effect even though individual material properties do not change markedly. The increase in α and decrease in s_t and k with temperature generally gives a lowering of R and R' at higher temperatures. At still higher temperatures,

Table VII. Strength of Ceramic Materials

Material	20°C.	400°C.	1000°C.
Al_2O_3	21,000	20,000	20,000
BeO	21,000	10,000	6,000
MgO	14,000	15,000	11,500
Mullite	12,000	10,000	7,000
Spinel	12,300	12,200	10,900
ThO_2	12,000	10,000	7,000
Zircon	12,000	10,000	6,000
ZrO_2 (stabilized)	20,000	17,500	14,800
Fused quartz	15,500	15,500	
Soda-lime-silica glass	10,000	10,000	
TiC	20,000	19,000	17,000
Porcelain	10,000	8,000	6,000
Fire-clay refractory	750	750	700
TiC cermet	160,000	155,000	140,000

[20] R. W. Douglas, "Thermal Endurance of Glass Articles," *J. Soc. Glass Technol.*, **20** [81] 517–23T (1936); *Ceram. Abstr.*, **17** [4] 139 (1938).

[21] J. H. Westbrook, "Thermal Shock Resistance of Metallized Ceramics," Sc.D. Thesis, Department of Metallurgy, M. I. T. (1949).

Table VIII. Thermal Stress Resistance Factors for Some Ceramic Materials*

Material	100°C. R (°C.)	100°C. R' (cal sec.$^{-1}$ cm.$^{-1}$)	400°C. R	400°C. R'	1000°C. R	1000°C. R'
Al_2O_3	37	2.7	36	1.1	40	0.60
BeO	33	17.3	31	6.9	14	0.69
MgO	22	1.9	24	0.94	26	0.45
Mullite	75	1.1	68	0.75	84	0.84
Spinel	32	1.15	32	0.77	32	0.45
ThO_2	51	1.3	47	0.66	37	0.30
Zircon	137	(2.2)	115	1.4	73	0.73
ZrO_2 (stabilized)	66	0.31	62	0.30	53	0.29
Fused silica	2500	9.5	2400	10.1		
Soda-lime-silica glass	94	0.38	94	0.43		
TiC	42	2.5	40	1.3	(40)	0.56
Porcelain	116	0.48	103	0.43	116	0.52
Fire-clay refractory	38	0.14	41	0.14	178	0.48
TiC cermet	208	(17.3)	200	(8)	198	(4)

* Values in parenthesis are estimated.

the decrease in E and development of plasticity cause a sharp increase in thermal stress resistance. In Table VIII, thermal stress resistance factors are calculated for a number of ceramic materials, and in Fig. 15 the measured and calculated change of thermal stress resistance with temperature is shown.

The necessity for two thermal stress-resistance factors depending on the rate of heat transfer is shown in Fig. 16, where the fracture temperature of several materials is plotted as a function of the surface heat transfer parameter. At low rates of heat transfer, the thermal conductivity is of considerable importance, whereas at high rates of heat transfer it becomes unimportant. Consequently, the order of thermal shock resistance of ceramic materials varies depending on the heat-transfer conditions. It is apparent that no one factor or listing of ceramics can be satisfactory as a "thermal endurance" index.

VII. Test Methods for Thermal Stress Resistance

A large variety of thermal stress tests have been employed in the past. They can be classified according to the method of establishing temperature gradients and by the method of assessing thermal stress resistance. Temperature gradients have been established by cyclic heating and cooling,[13(q), 22] by a single rapid heating or cooling,[2, 13(e)(n), 15(c), 23] and by the establishment of steady-state thermal stresses.[13(a)(d)(h)(r)]

Thermal stress resistance has been measured by loss of weight,[22(a) (b) (d), 23(a) (b) (c)] decrease in strength,[17(a), 22(c)] or decrease in elastic properties[17(a), 23(d)] after a specified treatment, or the severity of treatment necessary to cause a fracture[2, 13(a) (d) (e) (n) (q) (r), 15(c), 23(e) (f)] or a specified loss in weight, strength, or elasticity.[17(a)] The applicability of various tests depends mainly on the testing objective. Tests are generally designed either to give results which correlate well with specific service conditions, to determine the effect of variable properties, or to provide a general index of thermal shock resistance.

The most direct tests are simulated service tests such as the A.S.T.M. panel spalling tests[22(a) (b) (d)] and water quenching of glassware.[2, 15(c), 23(e) (f)] The advantage of this type of test is that results can be safely applied to a particular application (except that particular and fairly common service conditions, such as slag penetration in refractories and corrosion or impact failure of turbine blades, may void the practical results of the controlled tests). The major disadvantage is that a new test is necessary for any change in application conditions, and consequently it is an expensive procedure which can usually be justified only when the range of use conditions is well known. In this kind of test, cyclical testing is desirable because it accentuates test results. Ceramic materials may show static fatigue but, in general, show no ill effects from repeated loading below the elastic limit. With measurement of resistance by fracture, weakening, or weight loss, a number of cycles will increase initially small effects.

By employing short-term cyclic tests well above the thermal stress limit, the amount of weight loss can be considerably increased. However, there is no general relation between these results and the results at a lower thermal stress level which might actually be used in service. Variation in material properties and thermal stress conditions may vary the order of merit of different materials under different conditions, and these changes cannot be predicted without a knowledge of the individual factors involved.

Another widely employed test is the use of single thermal shock cycles of increasing severity until fracture occurs, measuring the temperature difference required to cause fracture or a specified decrease in strength or elasticity. In this kind of test, fractures may occur as small surface fissures so that it is essential to examine each specimen carefully for failure after each test. In this regard, decrease in strength and elasticity are helpful, particularly for porous materials or commercial refractories with some surface discontinuities, since surface fissures are difficult to observe. The variation of material properties with the temperature level, and the general lack of heat-transfer data, make general applicability of results to other conditions questionable. For a given temperature range, the order of merit of different materials should be valid.

Tests finding increasing application are steady-state tests of thermal stress failure. In general, the most convenient shape to employ is a hollow cylinder with interior heating. Results from these tests give an easily observable and definite fracture, since a steady stress is employed. The temperature level can be varied, and the effect of various factors affecting stress resistance can be investigated. Together with thermal conductivity data, general results for an order of merit over a range of conditions can be obtained. Due to the generally unknown variation in the factors affecting thermal stress failure under various conditions, results cannot usually be quantitatively applied to a specific application. In the author's opinion, this type of test to determine a general order of merit for a given application, together with a simulated test or trial to determine a quantitative basis for the order of merit, is probably the most fruitful approach to thermal stress testing. Tests with an essentially infinite value for the relative rate of heat transfer may give essentially the same results.

Another approach to thermal stress testing is the separate evaluation of α, E, s_f, k, and μ at various temperature levels.[13(a) (e)–(k)] Although these measurements are not

---

[22(a)] R. A. Heindl and W. L. Pendergast, "Panel Tests for Thermal Spalling of Fire-Clay Brick Used at High Temperatures," *J. Research Natl. Bur. Stand.*, **34** [1] 73–96 (1945); RP 1630; *Ceram. Abstr.*, **24** [5] 91 (1945).

(b) G. R. Eusner and W. S. Debenham, "Spalling of Fire-Clay Brick," *Bull. Am. Ceram. Soc.*, **31** [12] 489 (1952).

(c) C. W. Parmelee and A. E. R. Westman, "Effect of Thermal Shock on Transverse Strength of Fire-Clay Brick," *J. Am. Ceram. Soc.*, **11** [12] 884–95 (1928).

(d) A.S.T.M. Designation C-38-49, "Basic Procedure in Panel Spalling Test for Refractory Brick," A.S.T.M. Comm. C-8, 1952.

[23(a)] W. Steger, "Die Widerstandsfähigkeit feuerfester Baustoffe gegen Temperaturwechsel," *Stahl u. Eisen*, **45**, 249 (1925).

(b) A. C. Elliot and R. J. Montgomery, "New Type of Thermal Shock," *J. Can. Ceram. Soc.*, **6**, 44–48 (1937); *Ceram. Abstr.*, **17** [1] 20 (1938).

(c) R. A. Heindl, "Comparative Tests for Determining Resistance of Fire-Clay Brick to Thermal Spalling," *Proc. A.S.T.M.*, **31** [Part II] 703–14 (1931); *Ceram. Abstr.*, **11** [3] 184 (1932).

(d) Private communication from H. F. G. Ueltz and N. N. Ault, 1953.

(e) E. Seddon, "Proposed Standard Thermal Endurance Test Based on Use of Glass Rods. A Report of The Society of Glass Technology," *J. Soc. Glass Technol.*, **20**, 498–510T (1936).

(f) W. M. Hampton, "Thermal Endurance of Glass," *J. Soc. Glass Technol.*, **20** [81] 461–74T (1936); *Ceram. Abstr.*, **17** [4] 139 (1938).

simple, the general agreement between the order of calculated thermal stress resistance and measured values has been reasonably good.

VIII. Methods of Improving Thermal Shock Resistance

One important consideration in many applications is proper design to avoid large thermal stresses. Very often, techniques which avoid stress concentration factors, and designs which avoid restraints and allow for expansion of various parts of the structure, can improve thermal stress resistance. In some designs, the size of component parts can be reduced without loss of utility with a consequent reduction in thermal stresses.

Physical factors can, of course, be controlled to a certain extent. Strength increases are usually accompanied by an increase in the elastic modulus, with a variable resultant change in thermal stress resistance. For some materials, such as certain cermet compositions, the increase in strength may be considerably higher than the increase in E. Very often, a range in firing temperature or density will lead to a maximum value of s_f/E. The coefficient of expansion can also be controlled to a certain extent. Materials such as fused silica, zircon, SnO_2, Pyrex-brand glass, and Stupalith with low coefficients of expansion may contribute considerably toward better thermal stress resistance. The thermal conductivity can be improved by increasing density and purity. A few per cent silica in aluminum oxide may decrease the thermal conductivity by half.

The possibility of prestressing ceramic materials also offers an opportunity for increasing thermal stress resistance. Ceramic or metallic coatings,[21] thermal tempering, and other methods of prestressing are all worthy of further investigation. We were unable to find any reports in the literature of tempered dense ceramic oxides in the plastic range. We have heated some spherical samples of zirconia to 1600°C. and rapidly cooled them in air to develop compressive stresses in the surface. These samples withstood a water quenching Δt_f of 150° to 160°C., compared with 125° to 130°C. for samples which had not been heat-treated.